REFERENCE 24

R. CAIZERGUES, E. DEILGAT, P. LECORCHE, L. MAUBERT, AND H. REVOL, "CRITICALITY OF LIQUID MIXTURES OF HIGHLY ^{235}U-ENRICHED URANIUM HEXAFLUORIDE AND HYDROFLUORIDE ACID," (TRANSLATION) UNION CARBIDE CORPORATION REPORT Y-CDC-9 (MAY 1971).

Y-CDC-9

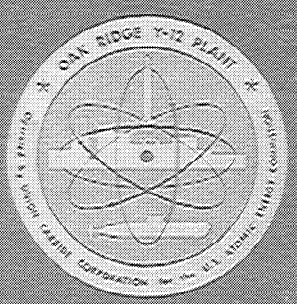

UNION CARBIDE CORPORATION
NUCLEAR DIVISION
OAK RIDGE Y-12 PLANT
operated for the
U.S. ATOMIC ENERGY COMMISSION

CRITICALITY OF LIQUID MIXTURES OF HIGHLY ^{235}U-ENRICHED URANIUM HEXAFLUORIDE AND HYDROFLUORIC ACID

Robert Caizergues, Edouard Deilgat, Pierre Lécorché,
Louis Maubert, and Henri Revol

Commissariat A L'Énergie Atomique
Direction de la Protection et de la Sûrete Radiologiques
Service D'Études de Criticite'

CRITICALITY DATA CENTER

Printed in the United States of America. Available from
National Technical Information Service
U.S. Department of Commerce
5285 Port Royal Road, Springfield, Virginia 22151
Price: Printed Copy $3.00; Microfiche $0.95

UC-46
Criticality Studies

Y-CDC-9

CRITICALITY OF LIQUID MIXTURES OF HIGHLY ^{235}U-ENRICHED URANIUM HEXAFLUORIDE AND HYDROFLUORIC ACID

Robert Caizergues, Edouard Deilgat, Pierre Lécorché,
Louis Maubert, and Henri Revol

Commissariat A L'Énergie Atomique
Direction de la Protection et de la Sûrete Radiologiques
Service D'Études de Criticite

Oak Ridge Y-12 Plant

P.O. Box Y, Oak Ridge, Tennessee 37830

operated for the **U.S. ATOMIC ENERGY COMMISSION**
by **UNION CARBIDE CORPORATION–NUCLEAR DIVISION**
under Contract W-7405-eng-26

Date Issued: May 1971 (in translation)
Date Issued: April 1968 (in French)

FOREWORD

The Criticality Data Center was established under the auspices of the U.S. Atomic Energy Commission for the development of methods allowing extension and application of data derived from experiments and from analyses to problems in nuclear criticality safety, as well as for the review and evaluation of the data themselves. A necessary part of this program is a medium whereby information germane to the intent of the Center is made available. This report series has been inaugurated for that purpose.

The first five reports were published by and identified with the Oak Ridge National Laboratory. Subsequent reports, however, issued from the Oak Ridge Y-12 Plant, are identified by a number sequence including the prefix Y-CDC.

Inquiries should be directed to E. B. Johnson, P. O. Box Y, Oak Ridge, Tennessee 37830.

Previous Reports in This Series:

ORNL-CDC-1 Criticality of Large Systems of Subcritical U(93) Components by J. T. Thomas (1967).

ORNL-CDC-2 Calculated Neutron Multiplication Factors of Uniform Aqueous Solutions of ^{233}U and ^{235}U by J. Wallace Webster (1967).

ORNL-CDC-3 Estimates of Maximum Subcritical Dimensions of Single Fissile Metal Units by W. H. Roach and D. R. Smith (1967).

ORNL-CDC-4 The Effect of Unit Shape on the Criticality of Arrays by J. T. Thomas (1967).

ORNL-CDC-5 Minimum Critical ^{235}U Enrichment of Homogeneous Hydrogenous Uranyl Nitrate by S. R. Bierman and G. M. Hess (1968).

Y-CDC-6 Some Effects of Interspersed Moderation on Array Criticality by J. T. Thomas (1969).

Y-CDC-7 Uranium Metal Criticality, Monte Carlo Calculations and Nuclear Criticality Safety by J. T. Thomas (1970).

Y-CDC-8 Use of Borosilicate Glass Raschig Rings as a Neutron Absorber in Solutions of Fissile Material by J. P. Nichols, C. L. Schuske, and D. W. Magnuson (to be published).

PREFACE

For the first time the Oak Ridge Criticality Data Center is privileged to publish data originating in a laboratory outside the United States. The Station Expérimentale d'Études de Criticité of the Commissariat A L'Énergie Atomique located at Valduc (France) has completed a valuable series of experiments with uranium hexafluoride in which the uranium was highly enriched in the ^{235}U isotope. These results describing critical parameters of a uranium salt when associated with relatively small quantities of hydrogen are an important adjunct to the parameters of aqueous solutions measured some years ago.

The UF_6 for the experiments was made available by the United States Atomic Energy Commission and through this medium the results are published in translation in the United States. The data first appeared in French in a CEA report identified as R.68.1 dated April 1968.

The Center acknowledges the permission granted by the Commissariat to report this research and is grateful to M. Lécorché for assistance in its publication.

CONTENT

FIGURE CAPTIONS

Figure

LIST OF TABLES

CRITICALITY OF LIQUID MIXTURES OF HIGHLY ^{235}U-ENRICHED URANIUM HEXAFLUORIDE AND HYDROFLUORIC ACID

Robert Caizergues, Edouard Deilgat, Pierre Lécorché,
Louis Maubert, and Henri Revol

ABSTRACT

The criticality of spherical and near-spherical volumes of liquefied UF_6-HF mixtures, in which the uranium was enriched to 93% in ^{235}U, in Monel containers having 4-mm-thick walls and surrounded by an effectively infinitely thick water reflector, has been investigated. The hydrogen-to-uranium atomic ratio of the mixture ranged between zero and eighty, the latter corresponding to a composition of about 1.23 mol % UF_6. The temperature of the mixture during the experiment was between 70 and 95°C.

Short extrapolations utilizing measured and calculated reflector, temperature, dimensional, and structural-material coefficients of reactivity and neutron multiplication data established the critical dimensions of spheres of the several compositions. It was observed, for example, that the critical mass of unmoderated UF_6 is greater than 165 kg of uranium and that the critical spherical diameter of UF_6-HF is greater than 450 mm over the range of concentrations explored. Critical masses as low as 8.8 kg of uranium were observed.

Monte Carlo and neutron transport theory calculations gave values of the effective neutron multiplication factor in reasonably good agreement with experiment.

INTRODUCTION

The nuclearly safe masses of enriched uranium as specified by the currently accepted criticality guides[1-3] and illustrated in Fig. 1 apply to metallic uranium or to suspensions of the metal in water for H:U atomic ratios between zero and infinity and to aqueous solutions of uranium salts for H:U ratios greater than 20.

The only guide available for compounds or mixtures of enriched uranium with H:U ratios between 0 and 20 is the dashed curve of Fig. 1. To our knowledge there are no experimental data on homogeneous, highly enriched uranium in the concentration range below 3.2 g of uranium/cm^3 for H:U ratios between 0 and 20. Indeed, the aqueous solutions of uranyl fluoride (UO_2F_2) utilized in the experiments[3-5] had a maximum uranium concentration of 0.8 g/cm^3 corresponding to H:U ratios greater than 20. Similarly, in the critical experiments[6] with aqueous solutions of uranyl nitrate [$UO_2(NO_3)_2$], the concentrations were even lower and the H:U ratios were greater than 60. In both cases the limits were set by the solubility of the salts.

There have been experiments with uranium hexafluoride[7,8] but only with slightly ^{235}U-enriched uranium. Experiments have also been reported[9,10] with materials having low H:U ratios and low uranium density; the uranium was enriched to 95.1% and 30% in ^{235}U. This material was a mixture of UF_4 and Teflon (CF_2), with a composition corresponding to UF_6C, compressed into cubes and assembled with similar cubes of polyethylene (CH_2) to achieve H:U ratios ranging between 0 and 220. Of course, since the heterogeneity resulting from this method cannot be neglected, its effect has been estimated theoretically. More recent experiments[11] at the Oak Ridge Critical Experiments Facility made use of a pseudo-homogeneous mixture (UF_4-paraffin) at a minimum H:U ratio of 4 using uranium enriched to 2 and 3% ^{235}U.

---

1. References are listed beginning on page 77.

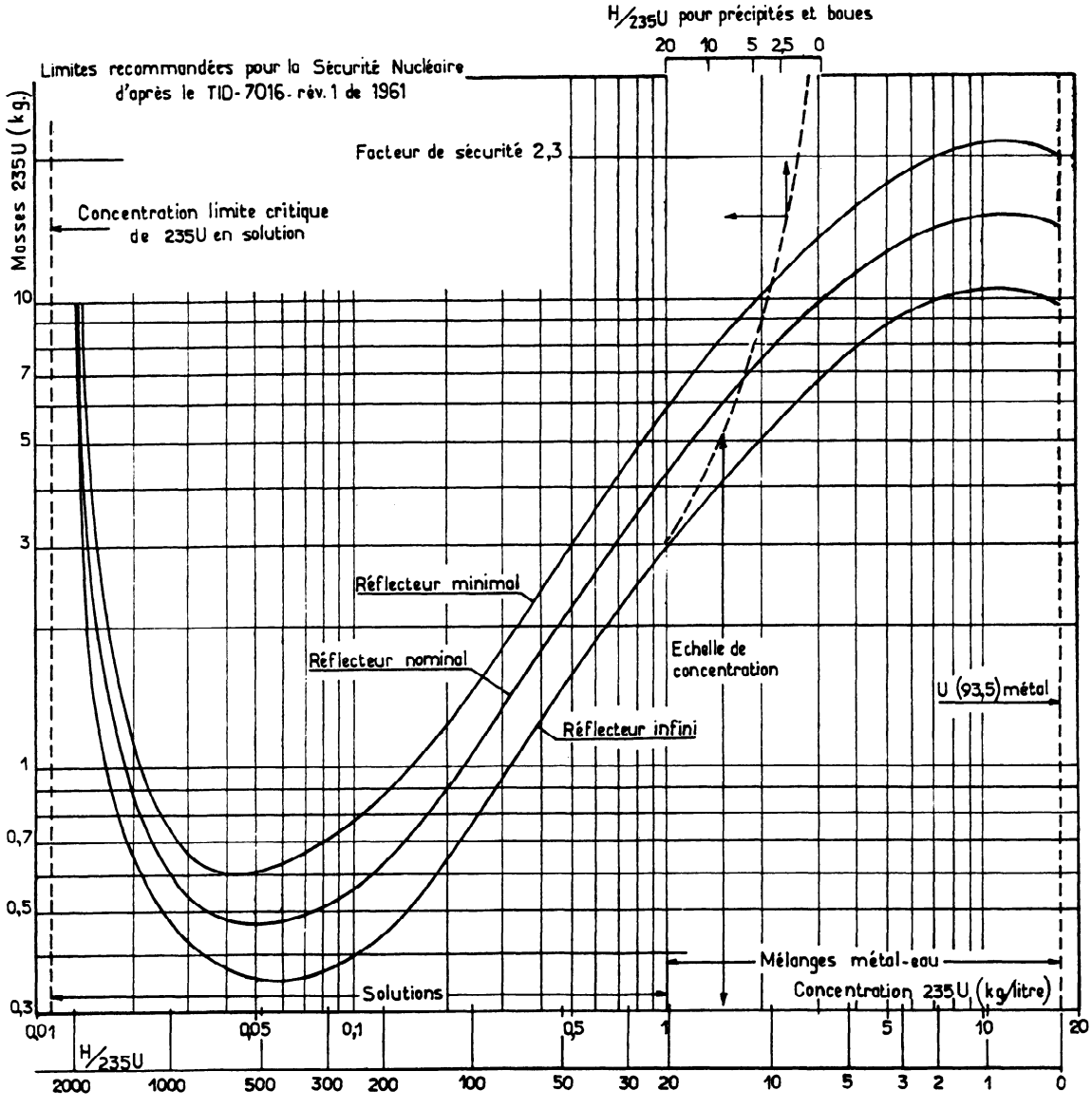

Fig. 1. Mass Limits for Single Spheres of Homogeneous Water-Moderated Uranium Enriched to 93% in ^{235}U.

The direct utilization of the above-cited experimental results with highly enriched uranium for setting realistic criticality specifications for uranium-bearing salts is difficult. Indeed, there is only one "homogeneous" point for which the concentration of fissile material is very high; the other points must be adjusted for the effects of heterogeneity.

As far as we know, the uranium hexafluoride-hydrofluoric acid mixture (UF_6-HF) is the only liquid with which high uranium concentrations and low H:U ratios may be obtained. This homogeneous material readily conforms to the shape of containers of simple geometry. The hydrogen-containing hydrofluoric acid possesses the same anion as the uranium hexafluoride and therefore does not affect the stability of the latter. In addition, UF_6-HF mixtures may be encountered under actual industrial conditions in processes involving uranium; i.e., isotopic separation by gaseous diffusion, nonaqueous recovery of reactor fuel elements, etc.

As a result of these considerations, the French Atomic Energy Commission decided to experimentally study the critical masses of UF_6-HF mixtures in the liquid phase at H:U ratios between 0 and 20. The actual experiments covered the range of H:U ratios between 0 and 80.

1. MATERIALS

1.1. Introduction

The preparation of homogeneous UF_6-HF in the liquid phase presents some rather complex technical problems. As a matter of fact, these liquid mixtures, in equilibrium with the gaseous phase, may only be prepared under certain specific conditions of temperature and pressure; otherwise, they may crystallize or separate into several phases.

In order to prevent crystallization, the mixture must be kept at a temperature above 65°C, the triple point of uranium hexafluoride. In order to avoid separation into several phases, i.e., to keep the mixture homogeneous, the temperature-pressure conditions must lie above the solubility curve of the phase diagram of UF_6-HF binary mixtures. Actually, for a certain range of values of H:U, the UF_6 and the HF are not miscible in all proportions except at temperatures higher than 103°C, which corresponds to pressures equal to or greater than 15 bars.

Although the physical characteristics of UF_6 and of HF are well known and have been published,[12-20] there are no available data on UF_6-HF mixtures. As far as we know, the only useful data are contained in the paper of Rutledge, Jarry, and Davis.[21] These studies disclosed the complex nature of the UF_6-HF system caused by the polmerization of the HF and, in addition to other results, made it possible for Jarry *et al.*[22] to establish the phase diagram of the mixture of these two materials, shown in Fig. 2, which was of great interest to us. Mixtures of these materials, within the bounds of certain ranges of temperature, pressure, and composition, exist as two immiscible liquid layers; this is the region immediately below the solubility curve of Fig. 2. Phase diagrams of this type are discussed by Glasstone.[23] However, in view of the scarcity of specific experimental data on the density of UF_6-HF mixtures, we decided to carry out some additional exploratory experiments.

Because of the highly corrosive nature of UF_6-HF mixtures, it was necessary to find a suitably resistant container material.

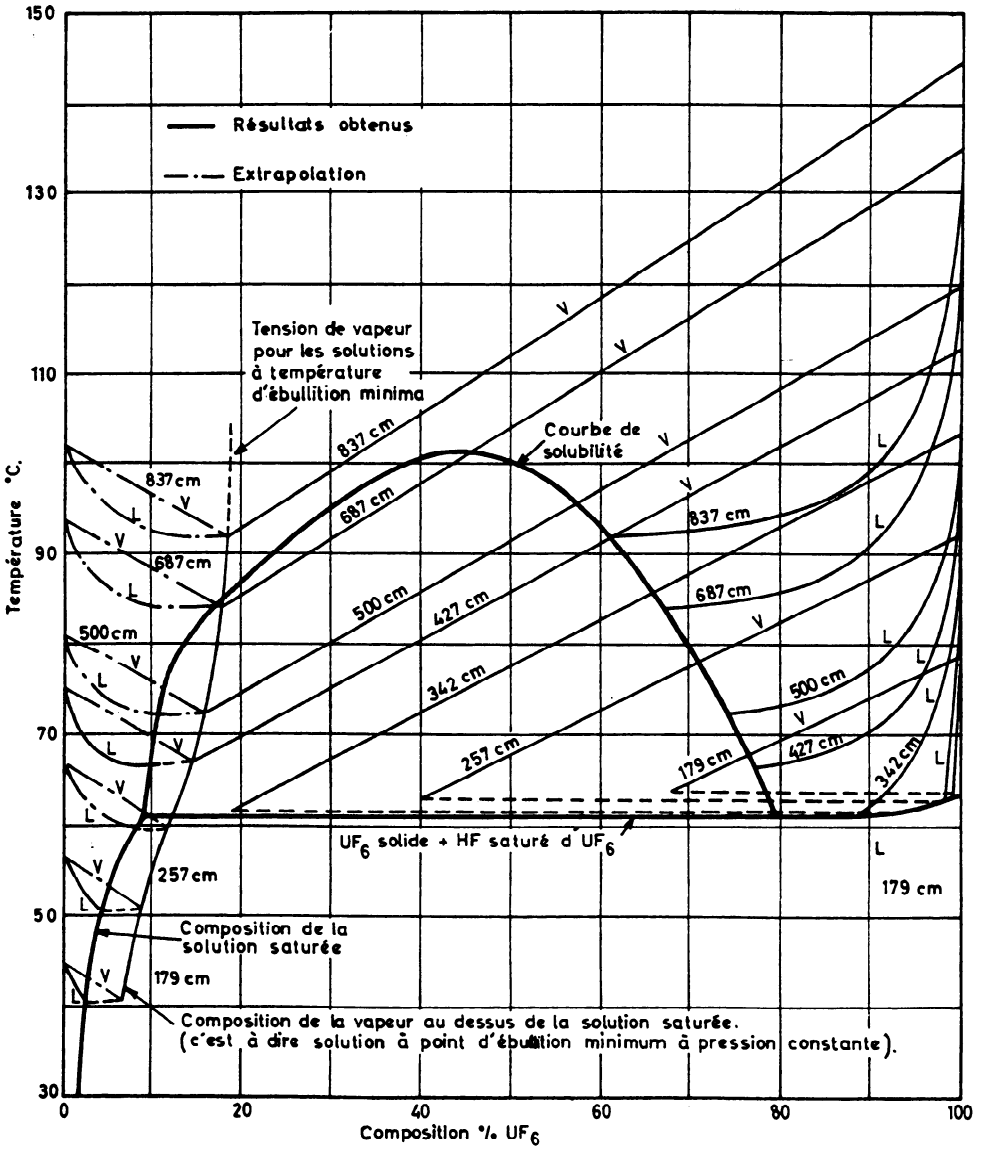

Journ. Phys. Chem. 57 (1953) 600

Fig. 2. Equilibrium Liquid-Vapor Phase Diagram for the UF_6-HF System.

These mixtures are also quite toxic, making precautions to protect personnel necessary. These two problems were solved by using Monel 400, by preparing strict construction specifications, and by enforcing rigorously the operating instructions.

1.2. Preliminary Experimental Studies

These preliminary experiments, by the Société de Recherches Techniques et Industrielles (SRTI), had several purposes:

a. the verification of the phase diagram of the UF_6-HF binary system and of the solubility curve;

b. the determination of the density of the mixtures as a function of temperature and composition;

c. the study of the homogenization of the mixture;

d. the investigation of various practical engineering problems, such as corrosion, the design and test of instrumentation for measuring pressure, temperature, and density, the development of sampling procedures, etc.

Although Jarry *et al.*[22] had studied these mixtures at temperatures between 40 and 104°C in concentration ranges quite close to the pure substances, the present study by SRTI included temperatures between 70 and 110°C and H:U ratios between 0 and 20; the results are given in Fig. 3.

The UF_6-HF mixture deviates clearly from the behavior of an ideal solution because it exhibits an azeotrope and a region consisting of two liquid layers, one HF and the other UF_6. This makes it impossible to calculate precisely the density of the mixture because the law of additivity of partial volumes does not apply. Therefore these densities were measured at H:U ratios between 0 and 20 with the equipment used for the study of the liquid-vapor equilibrium diagram. The results are presented in Fig. 4.

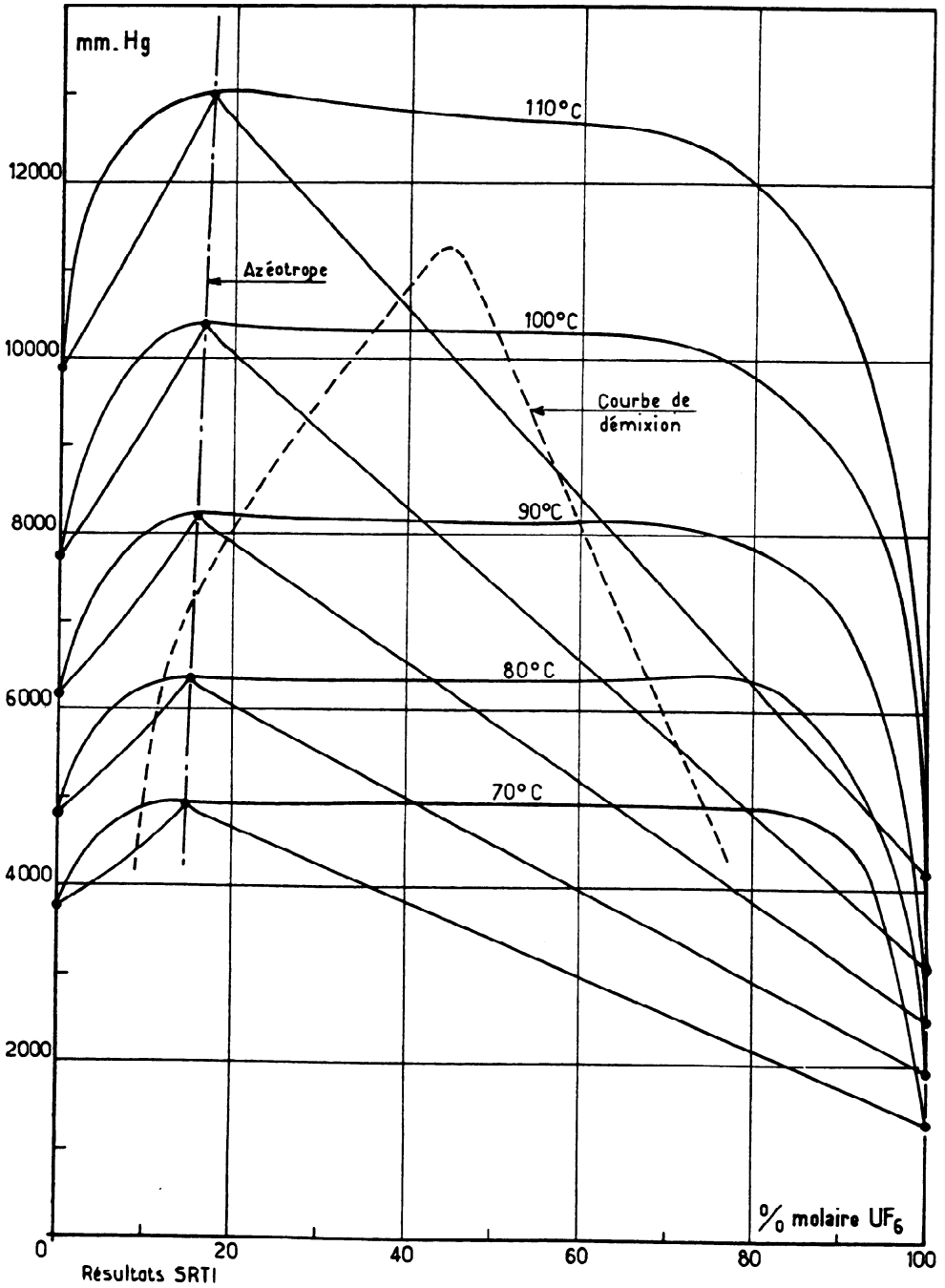

Fig. 3. Equilibrium Liquid-Vapor Phase Diagram for the UF_6-HF System.

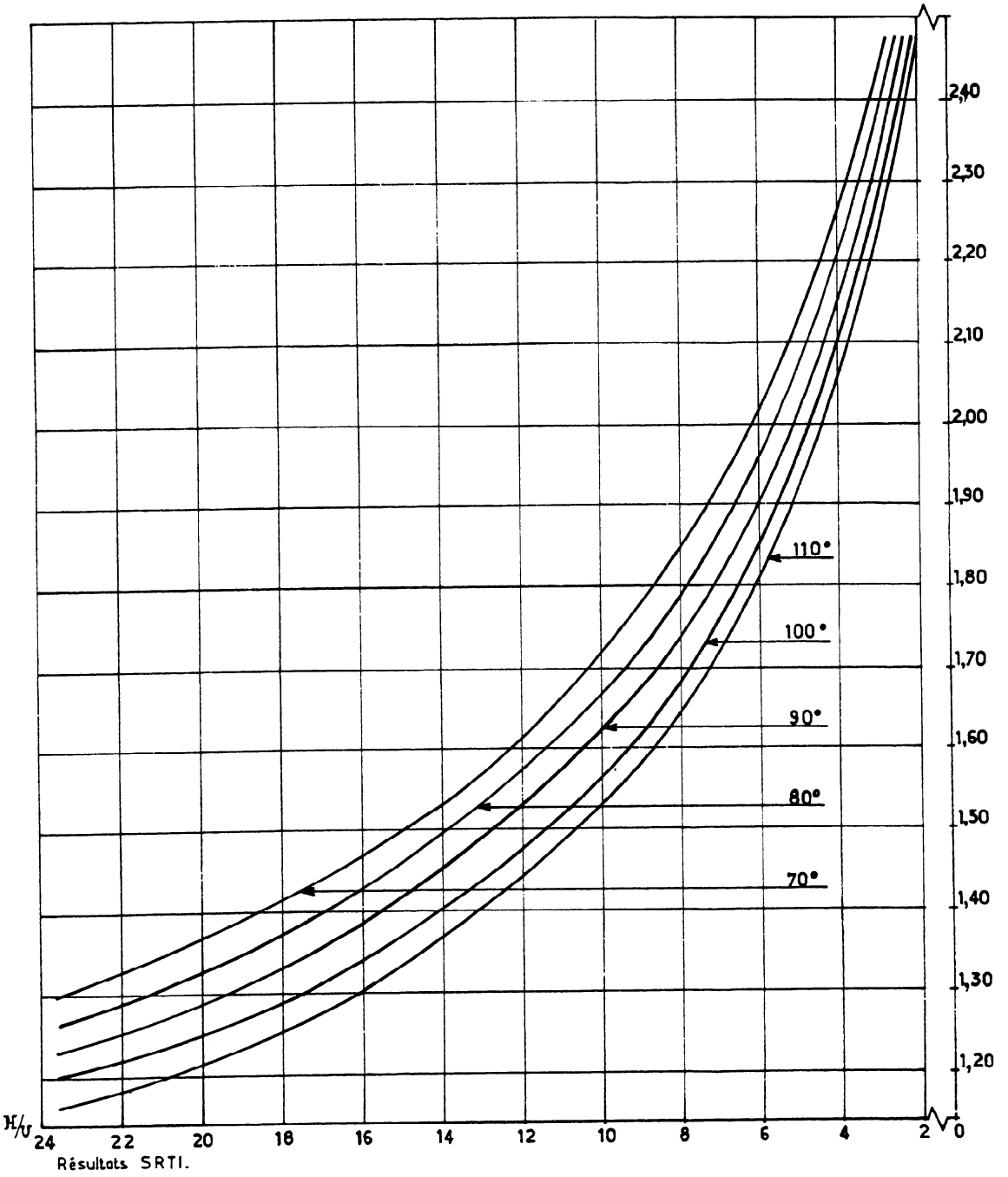

Fig. 4. Density of UF_6-HF Mixtures.

1.3. Design Requirements

Because of the existence of a region in which the two liquids are immiscible (Fig. 3), the equipment for criticality studies was designed to prepare homogeneous mixtures at preselected temperatures between 70 and 110°C and corresponding pressures between 3 and 17 bars; to homogenize the mixtures; and to control, in situ and during the experiments, all the physical characteristics of interest, such as pressure, temperature, and density.

2. EQUIPMENT

2.1. Location

The equipment occupied the western portion of the Station Expérimentale d'Etudes de Criticité of the Commissariat a L'Energie Atomique located at the Centre d'Etudes de Valduc. This Laboratory was described at the Stockholm Symposium.[24] The installation on the first floor, shown in Fig. 5 and including the main apparatus and the auxiliary equipment, was placed in a leaktight caisson with smooth steel interior partitions formed by demountable panels. The caisson was a rectangular parallelepiped, 16 x 8 x 8 m, contained within a larger concrete cell with 1.46-m-thick walls. Also on the first floor were a large room in which the equipment for the control of the experiment and for the display of measured quantities were centralized, an analytical laboratory, the controls for the auxiliary equipment, and a shop for surface treatment and decontamination.

Figure 6 is a plan of the basement which contained vessels for storing the mixtures following experiments, the cooling equipment, and various additional auxiliary equipment.

2.2. Description of the Systems

2.2.1 The Basic System. This apparatus, described in Figs. 7a, 7b, 7c, and 8, consisted of the mixing container, the core, and the drain tanks, listed in the order of the flow of the liquid UF_6 and HF from their storage containers. The mixing container and the core with its reflector tank were placed in a thermostated compartment, the temperature of which could be varied from 70 to 110°C. The drain tanks were located in the basement and the liquid was transferred to them by gravity.

2.2.1.1 The Core. Spherical geometry was chosen for the criticality studies of the UF_6-HF mixtures because of several advantages: it has a lower critical mass than other geometries, it provides a simple model for theoretical studies, and a spherical container is a good pressure vessel.

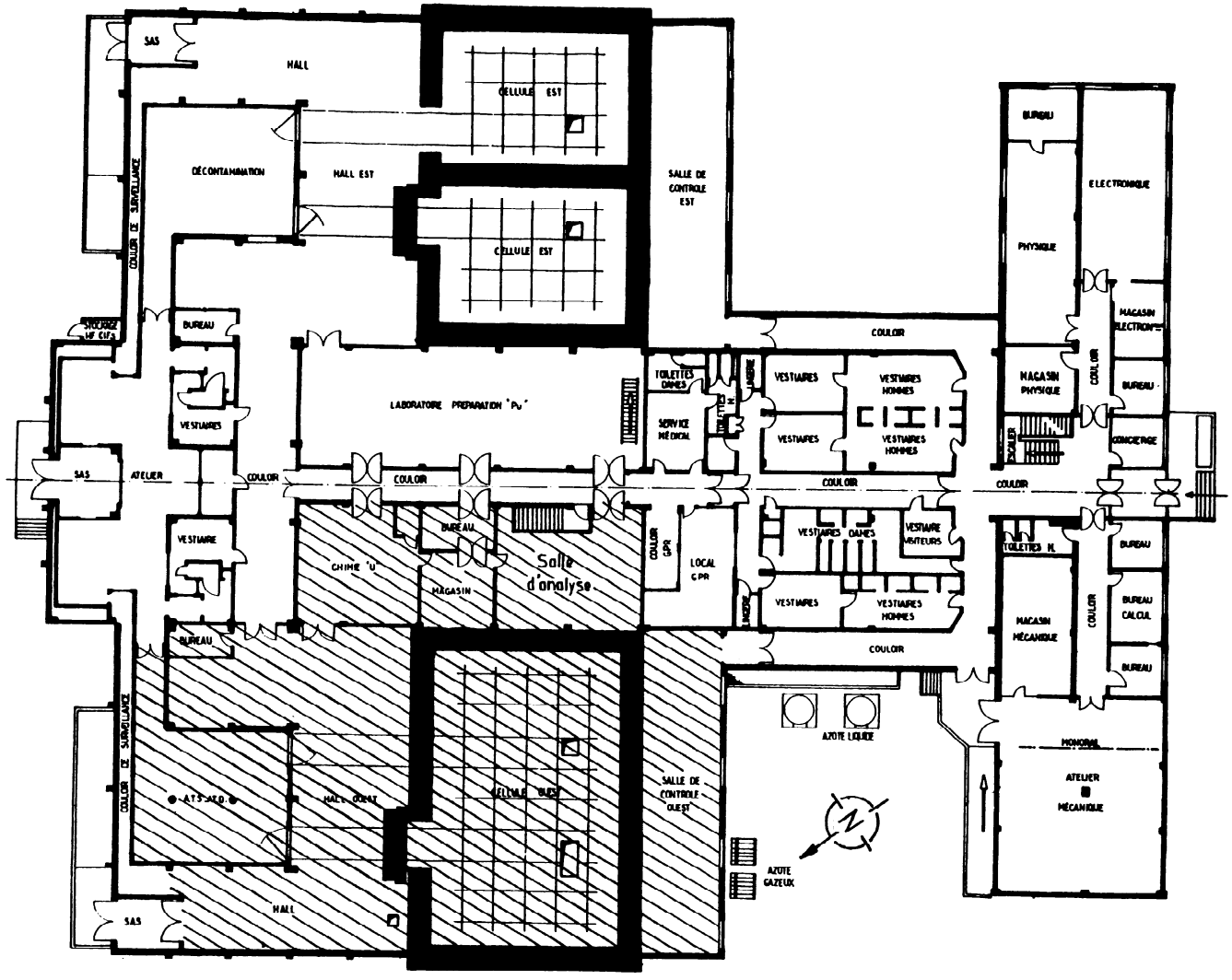

Fig. 5. Plan of the Ground Floor of the Building in Which the Experiments were Performed.

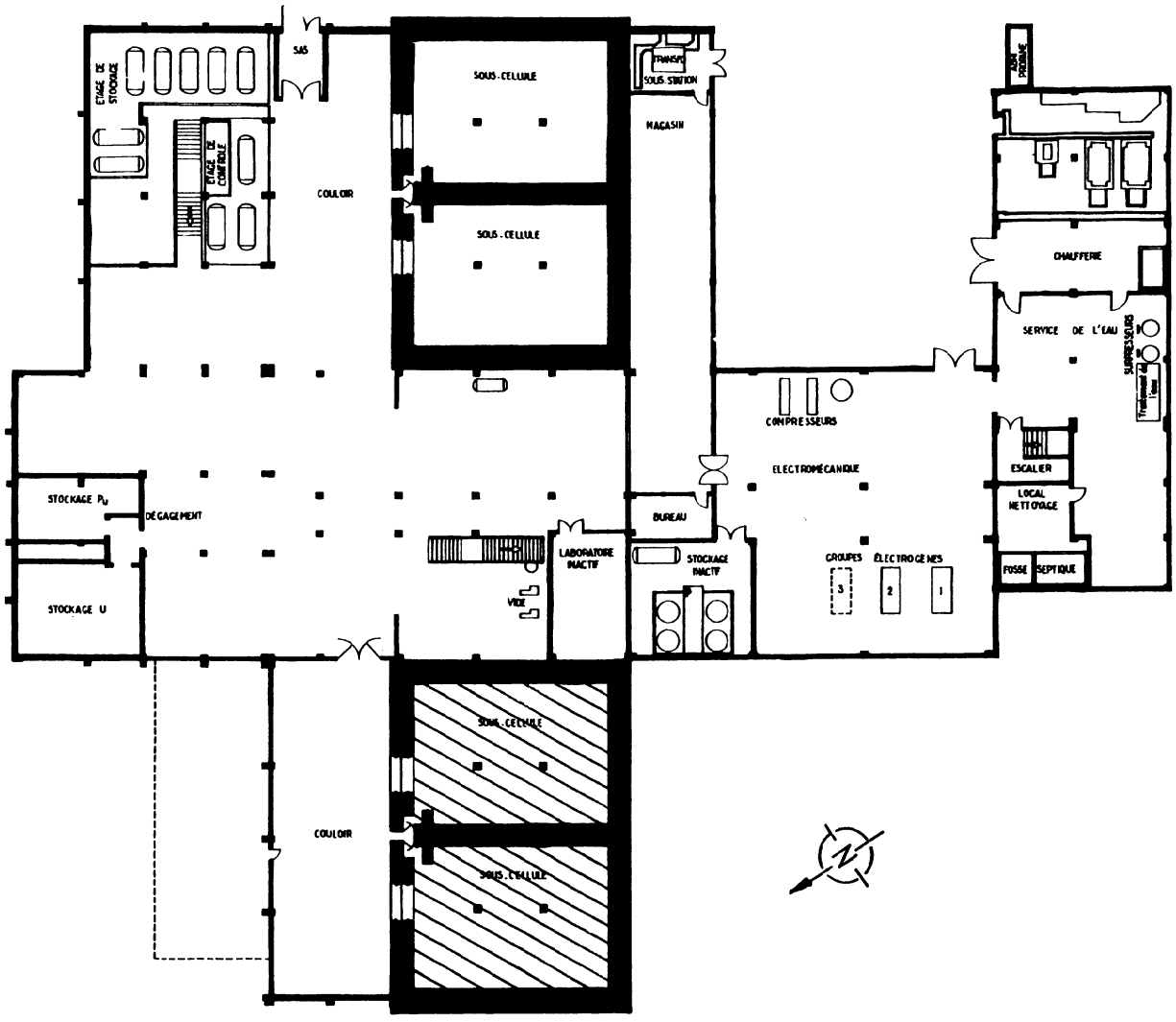

Fig. 6. Plan of the Basement of the Building in Which the Experiments were Performed.

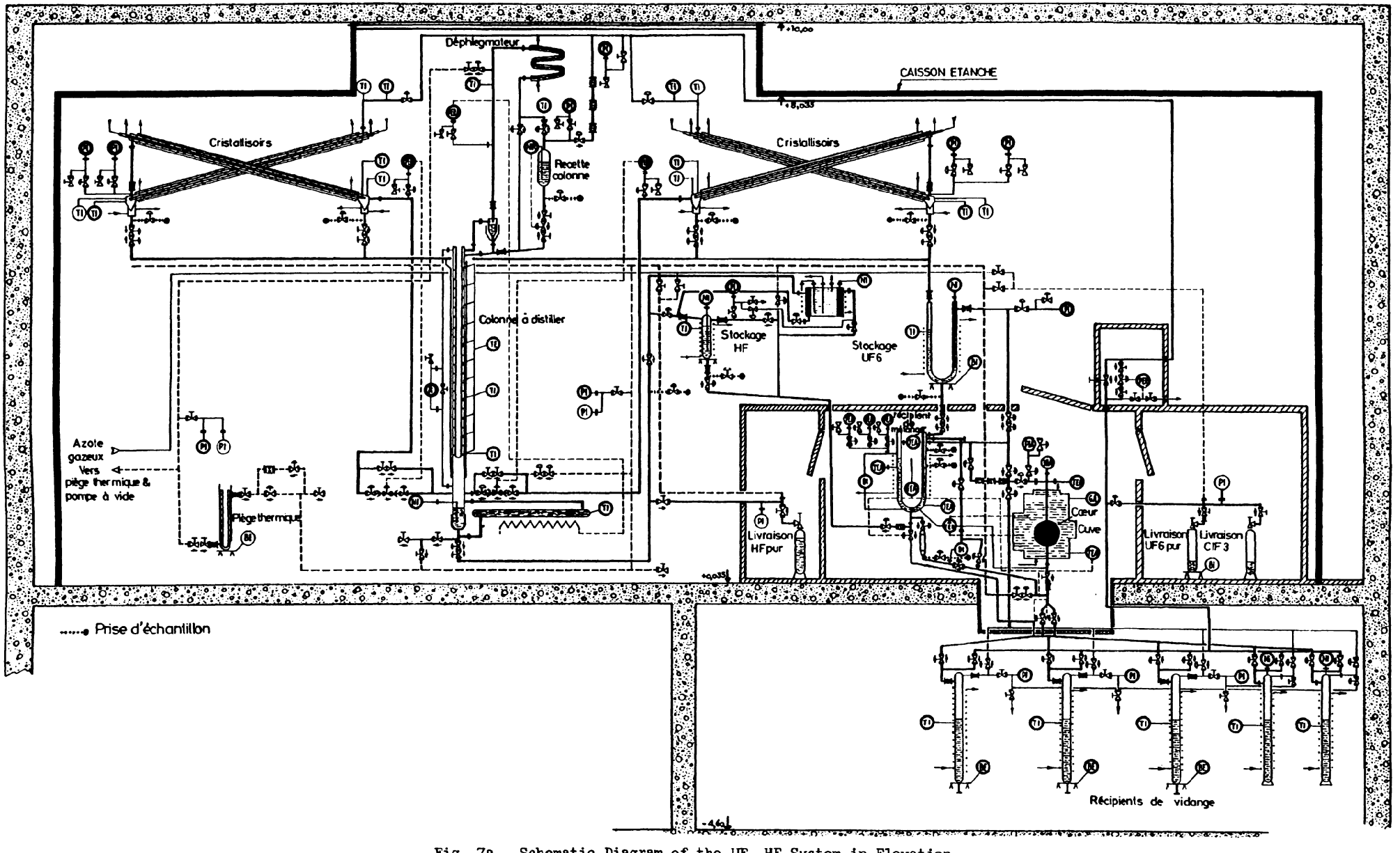

Fig. 7a. Schematic Diagram of the UF_6-HF System in Elevation.

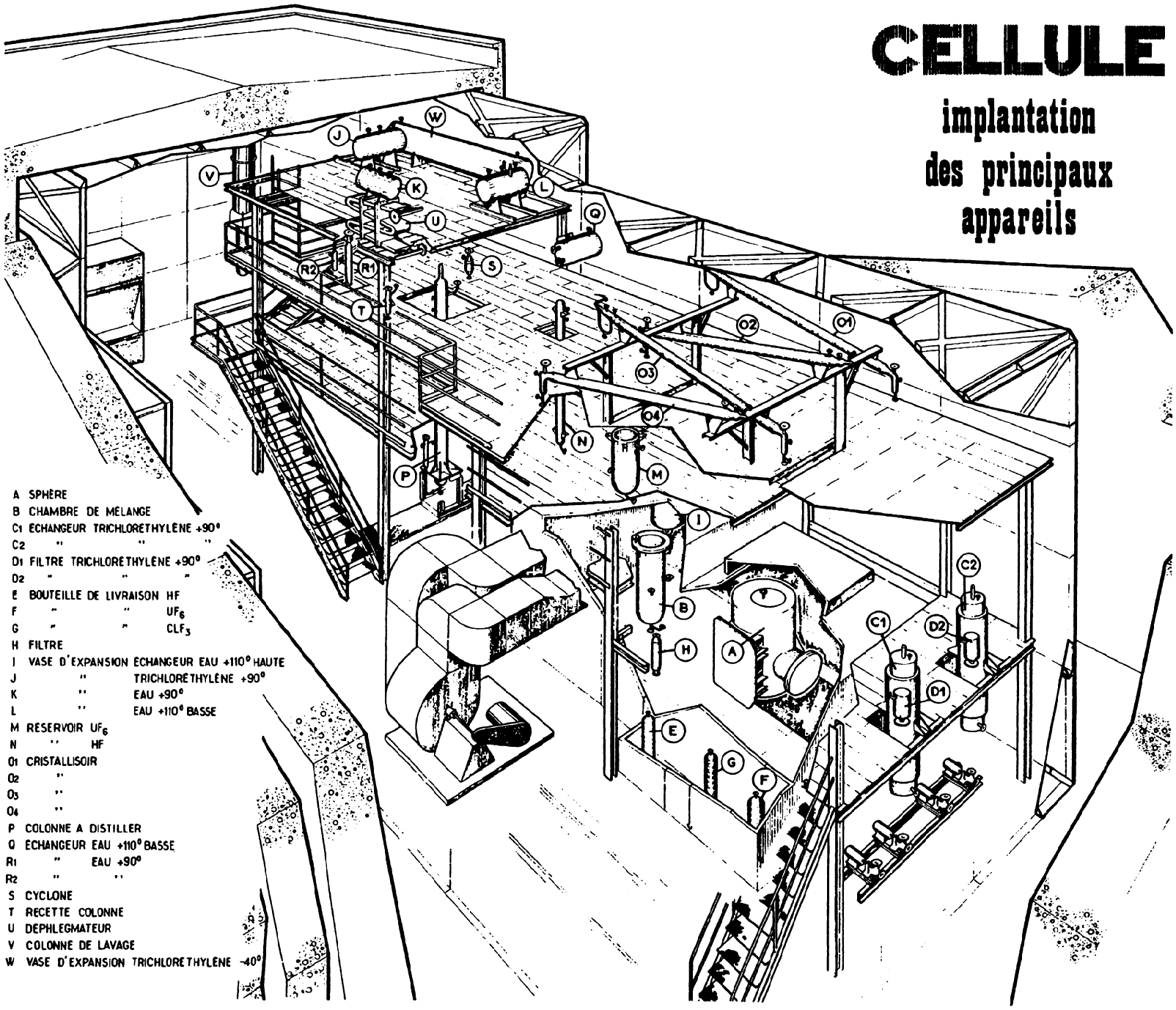

Fig. 7b. Diagram of the Cell Showing the Location of the Principal Apparatus.

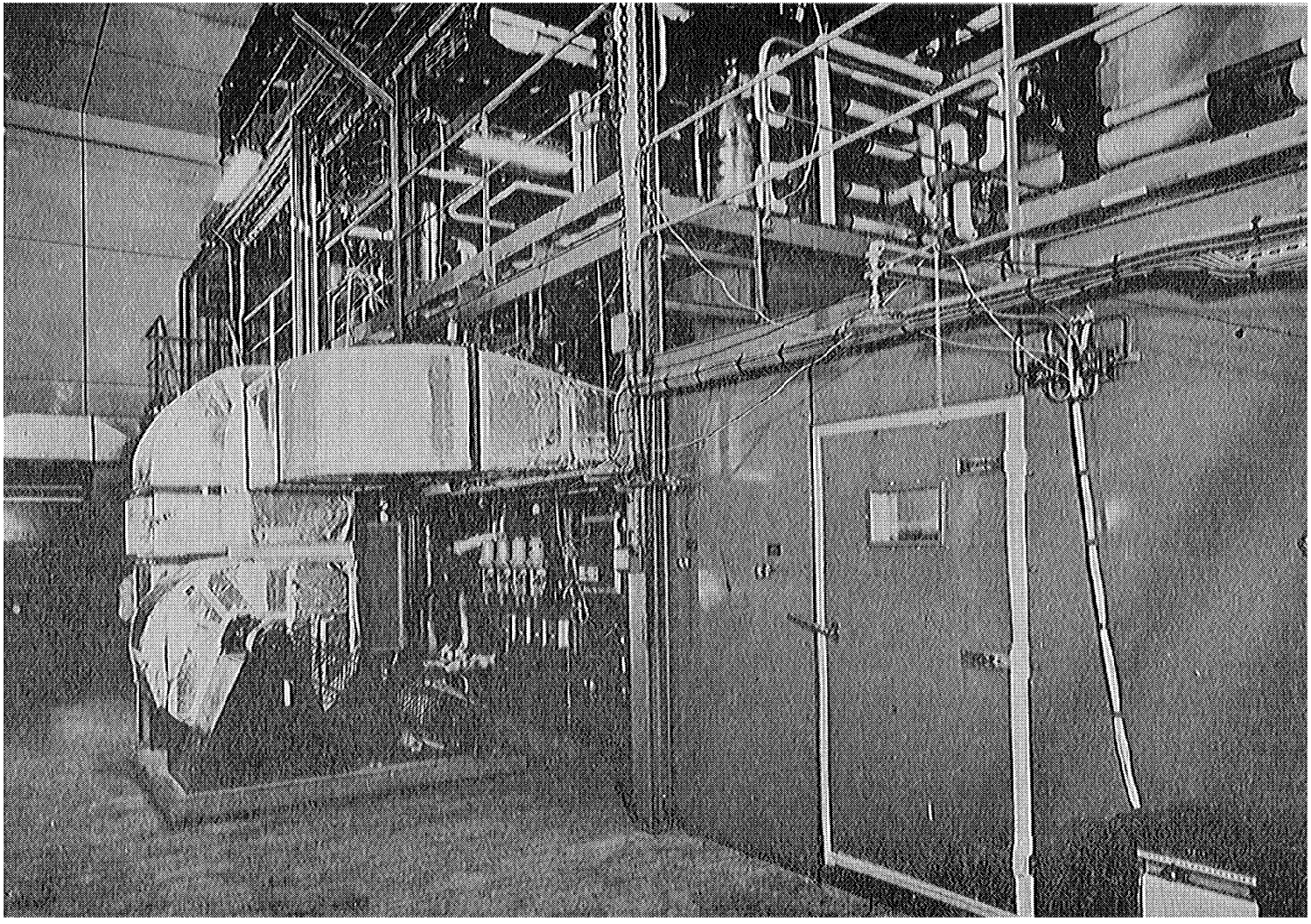

Fig. 7c. General View of the Apparatus in the Cell.

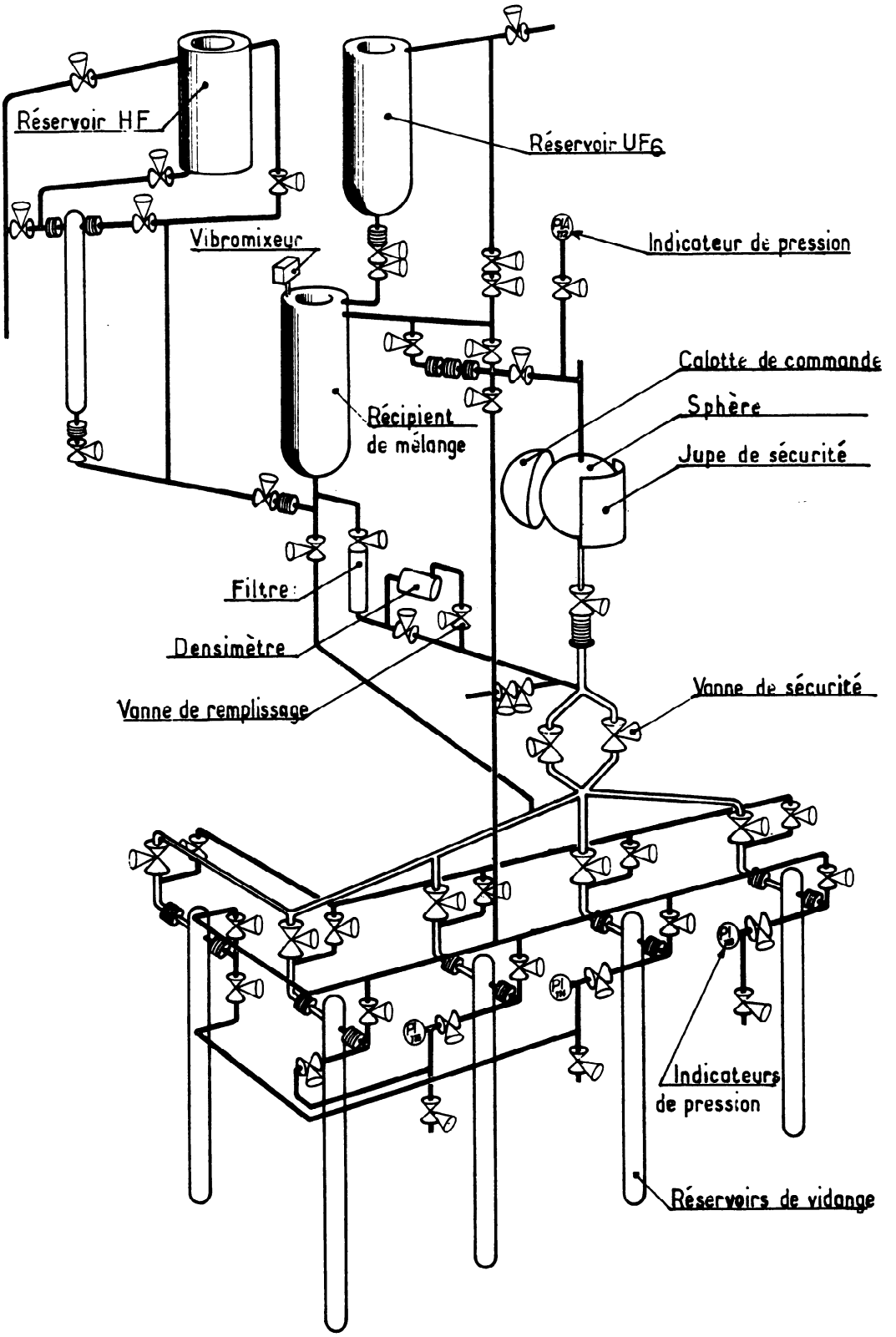

Fig. 8. Schematic Diagram of the Experiment System Showing the Principal Components.

Thus the core consisted of a Monel sphere provided with a vent at the top and systems of piping, from the storage and to the drain, at the bottom. A temperature-measuring device was located in the lower piping; the upper piping also contained a temperature probe, a pressure-measuring instrument, and a level-measuring device. An experimental sphere is shown schematically in Fig. 9a and as a photograph in Fig. 9b. The design was such that spheres of different size could be installed conveniently. Four spheres, with diameters of 400, 450, 510, and 540 mm, each having a 4-mm-thick wall, were used successively.

2.2.1.2 The Reflector Tank. The reflector tank, shown schematically in Fig. 10a and as a photograph in Fig. 10b, was a steel cylinder having inside dimensions of 1010 mm diameter and 1235 mm height, certified for a pressure of six bars. It was provided with access ports and flanges for introducing neutron counters and ionization chambers for measurements and for safety. The tank was filled with water which served as a reflector of neutrons and as a regulator of the temperature of the UF_6-HF mixtures.

2.2.1.3 Control and Safety Devices. These devices consisted of two separate systems shown in Fig. 10a: a) a spherical segment, which formed the control system, consisted of a 1-mm-thick cadmium foil sandwiched between 1- and 5-mm-thick stainless steel sheets, the thinner one being nearer the core; a geared-down motor, placed outside the tank and operated remotely from the control room, allowed positioning of the spherical segment with a precision of 1/3 mm at any desired distance from the sphere; b) a safety skirt consisting of a section of a cylinder of construction identical to that of the spherical segment. This safety skirt could be dropped, automatically by the safety system or manually, tangentially against the sphere. An electromagnetic lifting device could return the safety skirt to its original position after a drop.

2.2.1.4 The Mixing Container. The homogeneous mixtures of UF_6-HF having the desired concentration and temperature for the criticality experiments were prepared in a double-walled Monel vessel (Fig. 8) having a capacity of 130 ℓ. The interior cavity was lined with cadmium foil and was filled with water from the reflector-tank supply. The

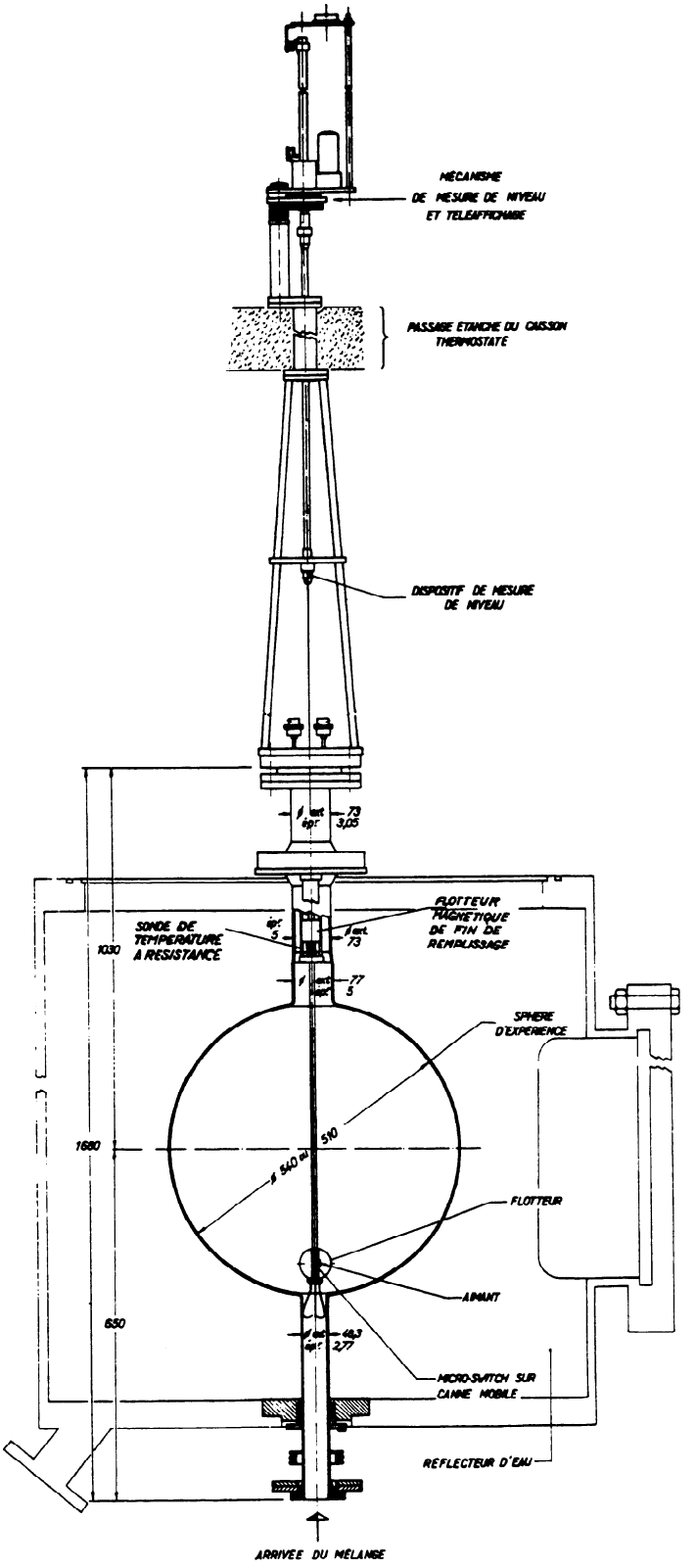

Fig. 9a. A Typical Experimental Sphere.

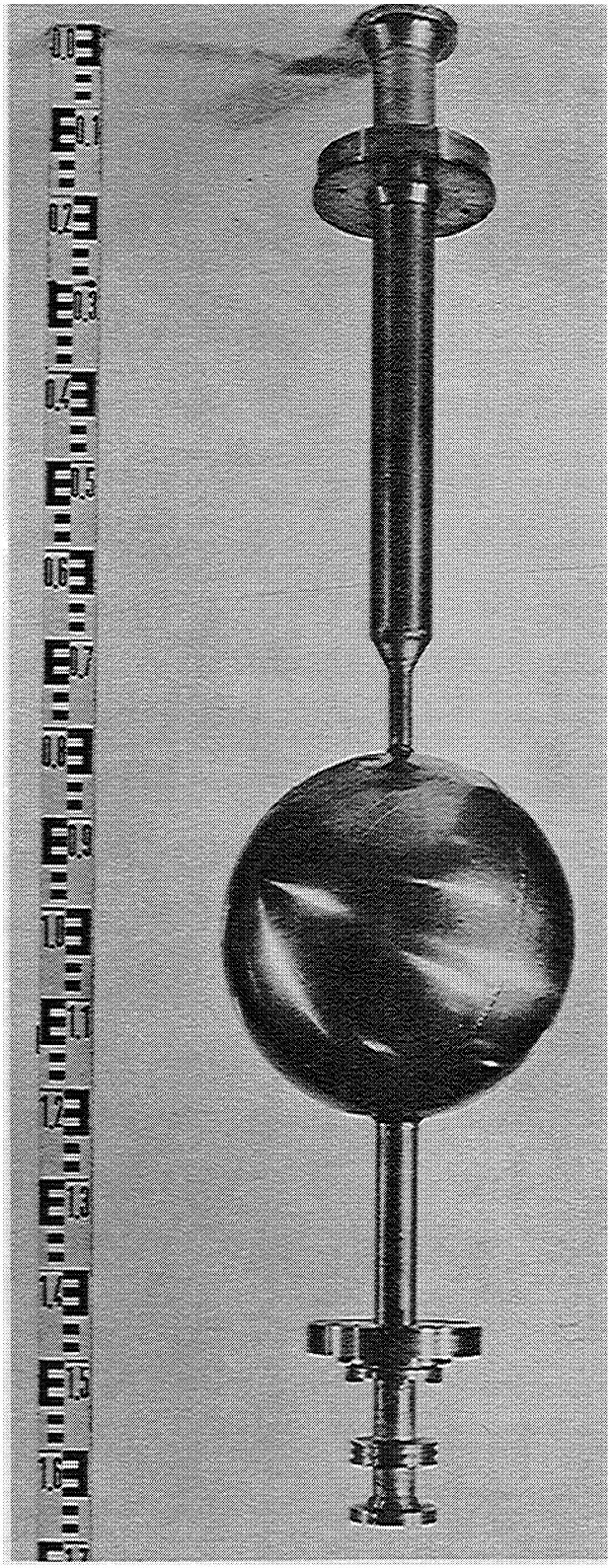

Fig. 9b. Photograph of an Experimental Sphere.

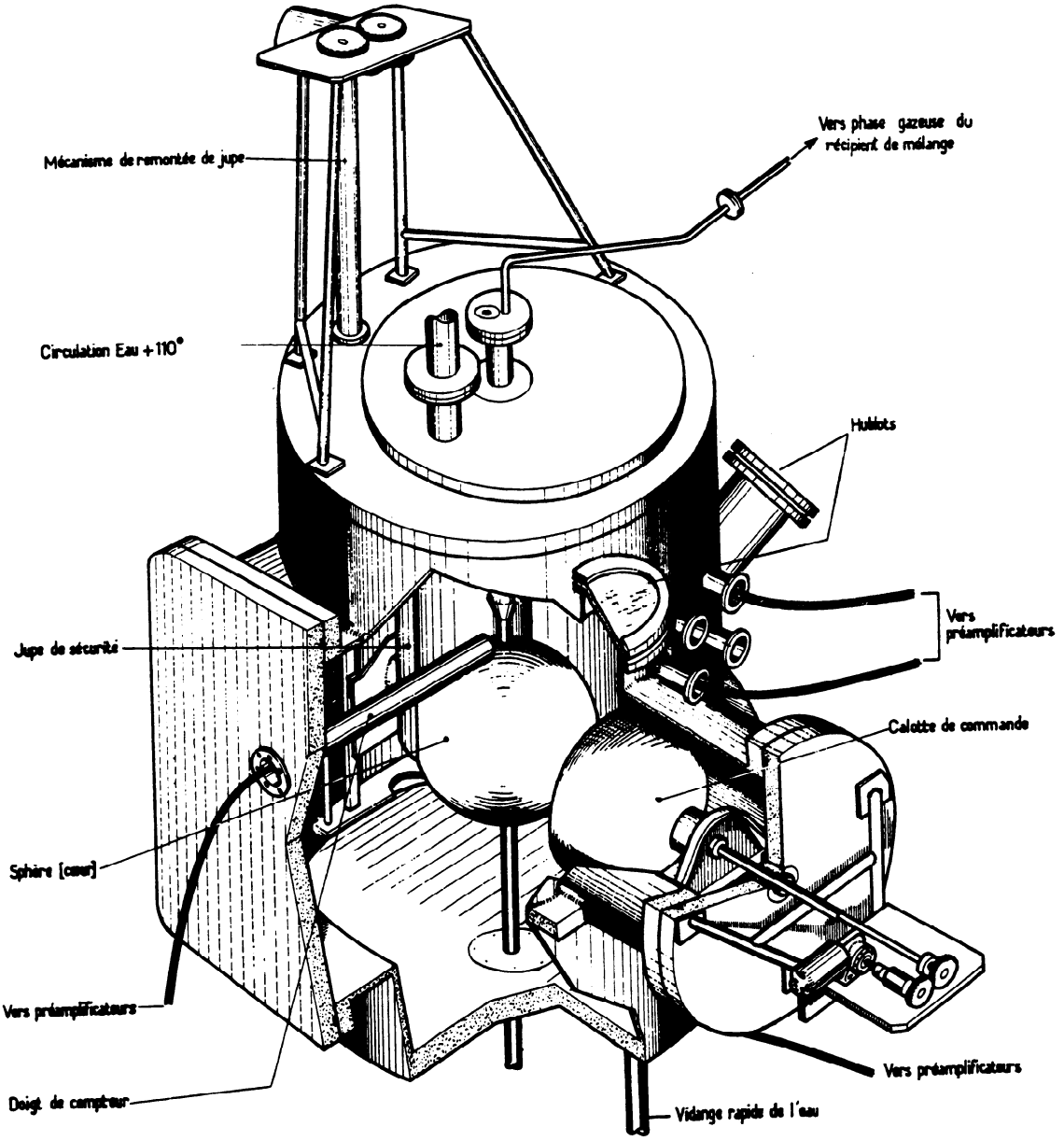

Fig. 10a. Diagram of a Sphere Installed in the Reflector Tank.

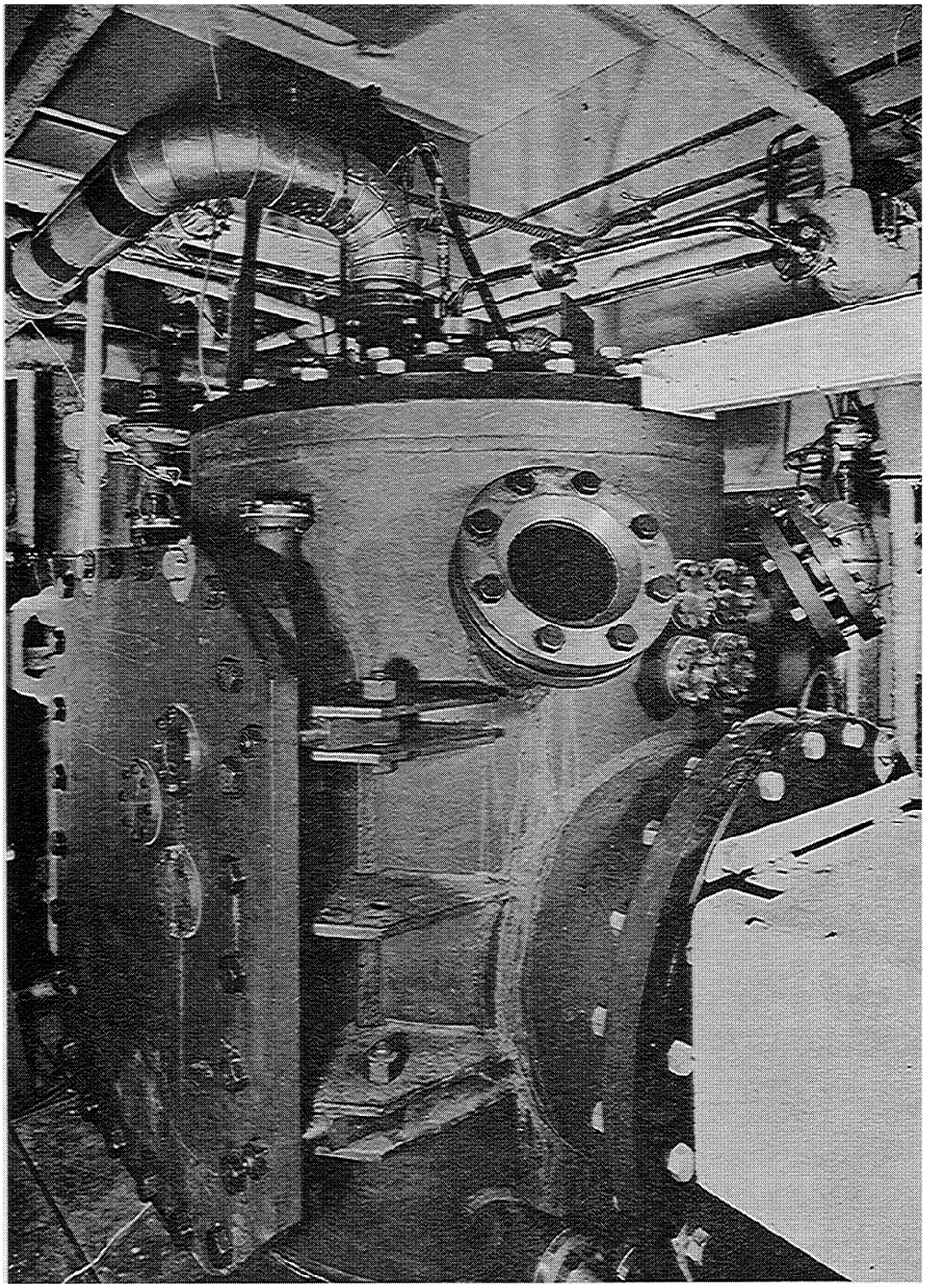

Fig. 10b. Photograph of the Reflector Tank.

container, which also served as the reservoir for filling the sphere, was provided with a homogenization device consisting of vibrating blades (a SRTI vibratory mixer) and with various measruing instruments which will be described in Section 2.3 on instrumentation.

2.2.1.5 Temperature Control. This whole system, consisting of the sphere, the control and safety devices, the reflector tank, and the mixing container, was placed within a 100 m^3 thermostated chamber. At all points within this chamber, the temperature was maintained at the required value between 70 and 110°C, with a precision of ± 1°C, by means of hot air circulating at a rate of 24,000 m^3/hr.

The sphere was maintained at the desired temperature by the reflector water which circulated continuously within the reflector tank. The water temperature was regulated by the inflow of hot water, produced by a resistance heater, on the basis of information from a temperature-measuring probe.

The temperature of the annular mixing container was kept equal to that of the sphere to within ± 0.3°C by a common hot water supply. The water circulated through a serpentine tube outside the mixing container and through its central interior cavity. A reheater and a cooler completed the circuit. This temperature equality was maintained by a differential temperature regulator and resistance probes immersed in the UF_6-HF mixture in the two vessels, which operated either the reheater or the cooler as required. This close control of the temperature of the mixture minimized the variation of the level of the UF_6-HF mixture in the sphere when it and the mixing tank were connected during an approach to criticality.

2.2.1.6 Drain Tanks. A system of rapid drainage allowed the removal of the UF_6-HF mixture to a storage system consisting of five Monel cylinders, 126 mm in inside diameter, located in the basement and shown schematically in Fig. 8. The reflector water could also be rapidly drained into a container in the basement.

2.2.2 The Separation and Storage Systems. The equipment for separating the mixture into UF_6 and HF and storing them preparatory to the next experiment is described in Fig. 7a.

2.2.2.1 Separation. For this operation the drain tanks were used as evaporators and were heated to 110°C by circulating hot water. The gaseous UF_6-HF mixture was subjected to fractional crystallization, the gas passing through a series of crystallizers cooled to -40°C by trichlorethylene. The output of these crystallizers was connected to a column kept at -180°C by an automatic liquid nitrogen system. Uranium hexafluoride was retained in the crystallizers and HF, containing traces of UF_6, was trapped in the column. The crystallizers were then reheated to 90°C by circulating hot trichlorethylene and the UF_6 was transferred thereby to its storage container.

In order to obtain pure HF, the traces of UF_6 were extracted from the mixture in the column by distillation. The column, which had served as a cold trap for the fractional crystallization, was used as a distillation column in this second phase. An electrically heated boiler and a dephlegmator, cooled by circulating water, completed the apparatus. The azeotropic UF_6-HF mixture, formed at the head of the column upon achieving equilibrium, was removed by repeated draining of the system. At the end of the operations, the pure HF at the bottom of the column was transferred by pressure into its storage container.

2.2.2.2 Storage. The 85-ℓ-capacity UF_6 storage container was located under the crystallizers from which it received the liquid UF_6 by gravity flow. This storage container was similar to the mixing container and could be heated to 90°C or cooled to -40°C. In order to control the amount of material transferred to the mixing container, provision was made to continuously weigh the storage container, an operation facilitated by the flexibility of all connections to it.

The HF was stored in two containers: one a fixed annulus of about 80-ℓ capacity and the other a cylinder of about 20-ℓ capacity equipped with flexible connections and a weighing apparatus; the latter container provided a means for introducing the appropriate mass of HF

into the mixing container in preparation for an experiment. The container was heated by 110°C circulating water.

2.2.3 Auxiliary Systems. In order to prepare the mixtures, to carry out the experiments, and, finally, to separate the components of the mixture, the operation of a number of devices, designated as auxiliary equipment, was required. They provided necessary heating, cooling, transfer of materials, ventilation, etc. They will not be described in detail and only the more important ones will be listed. They include:

a. a liquid nitrogen system supplied from two 5000-liter containers;

b. a system supplying trichlorethylene at -40°C; the trichlorethylene was cooled by compressors, operating with Freon 22, having a capacity of 16,500 kilocalories per hour;

c. a system supplying trichlorethylene at 90°C, which was heated by a 20-kW electric heater;

d. a system for supplying hot water at a temperature of about 110°C for heating the UF_6 and the HF storage containers and the drain tanks; it was provided with a 20-kW electric heater;

e. a 6-kW, 90°C hot water system for the dephlegmator of the distillation column;

f. 25-kW electrical resistance heaters wrapped around the pipes through which the UF_6-HF mixture flowed;

g. a gaseous-nitrogen system;

h. a high-quality compressed-air supply for the remote control and transmitter systems;

i. a system for routine ventilation of the caisson;

j. an emergency ventilation system;

k. a vacuum system for the removal of noncondensable gases from the entire UF_6-HF system and for the calibration of the pressure transducers; it consisted of a cold trap, a chemical trap, a bank of vacuum pumps, and a scrubbing column;

l. equipment for surface treatment and cleaning of the Monel pipes and containers before initial assembly and for decontamination when modifications were made.

2.3. Instrumentation

Separate sets of control instrumentation were installed for the operation of the critical experiment itself, for the separation of the components of the UF_6-HF mixture, and for the operation of the auxiliary apparatus.

All of the equipment was remotely operated from the control room, shown in part in Fig. 11, which was separated from the experiment cell by a 1.46-m-thick concrete wall. An electrical interlock system kept the cell access doors, each of 0.73-m-thick concrete, closed and locked during an experiment. These doors slid one behind the other so that the total thickness of concrete was 1.46 m when both doors were closed.

Displayed in the control room was information from the neutron sensors, including those in the safety channels, the health physics monitors, the indicators of the physical properties of the mixture, and the flow diagrams for the various fluid systems. Also available to the operators were actuators for the valves, the safety skirt, and the spherical control segment.

Finally, the following lockout and automatic systems were installed to provide maximum safety: electric interlocks to prevent errors on the part of the operators, such as unintentional flow of the mixture into the sphere, improper mixing of the components, etc.; and automatic programming to verify before starting an experiment that the instrumentation operated safisfactorily and the safety devices functioned reliably.

2.3.1 Physical Measurements

2.3.1.1 Pressure. Twenty pressure sensors located at various points in the system were connected to pneumatic or electronic transducers to either indicate the pressure or to transmit it to the control system as a command for action. These instruments had a precision of about 2%. The pressure of the mixture was measured by a null method utilizing a differential pressure pickup and a manometer precise to ± 0.1%. The pressure to be determined was applied to one side of the diaphragm of the differential pressure pickup and counteracted by nitrogen pressure on the other side; the nitrogen pressure was

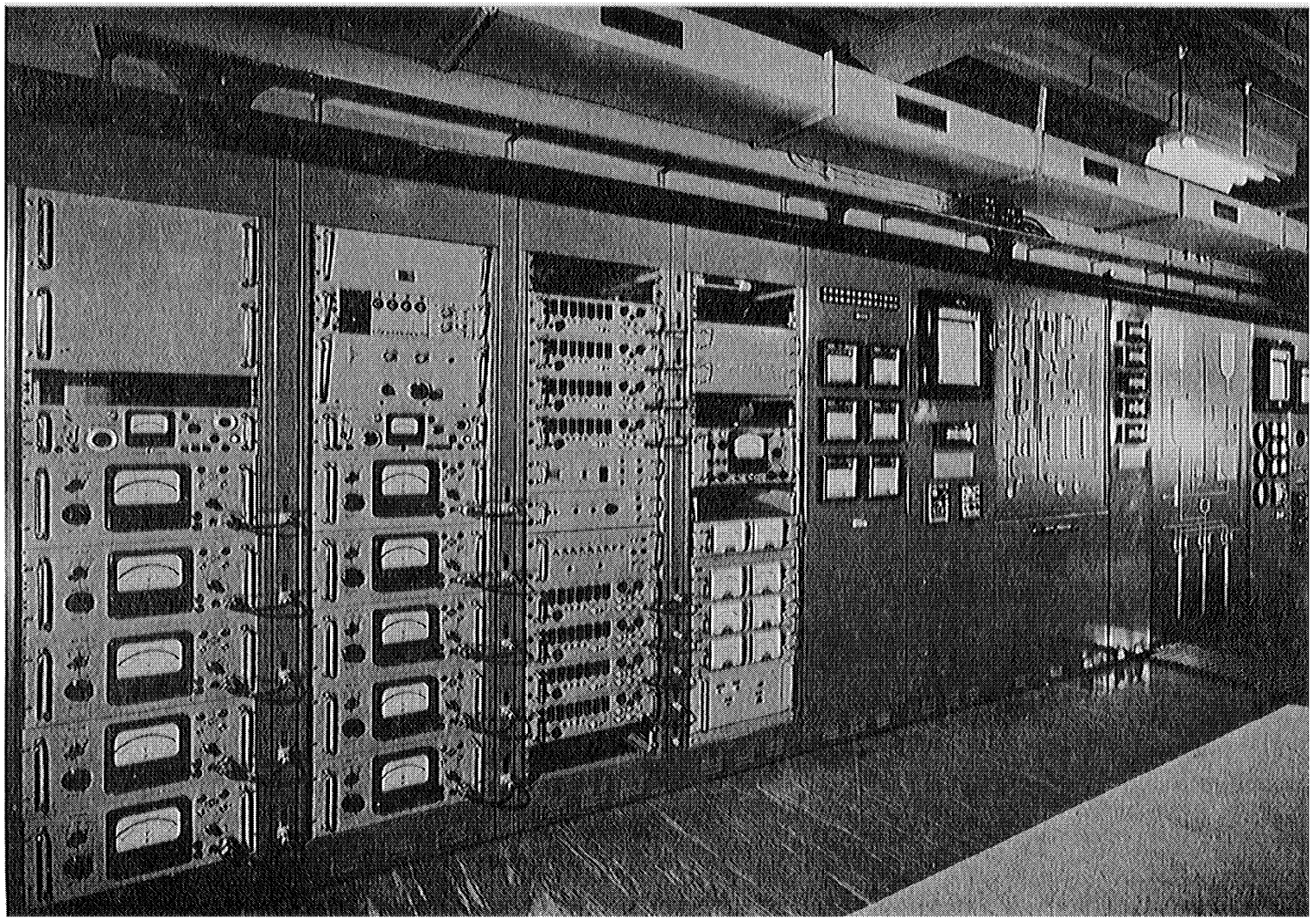

Fig. 11. Photograph of the Control Room.

determined by the manometer. The equilibrium position of the diaphragm was controlled automatically. The system allowed measurement of the pressure of the mixture in the sphere within ± 0.3%.

2.3.1.2 Temperature. Several remotely recording temperature-measuring devices were placed within the system. One of these, a resistance thermometer, shown in Fig. 9a, recorded the temperature of the UF_6-HF mixture.

2.3.1.3 Density. The density was measured continuously while the UF_6-HF mixture was flowing into the sphere, by means of a SEAM-type densitometer in the line from the mixing container to the sphere as shown in Fig. 8. The densitometer (see Fig. 12) weighed a fixed volume of liquid by means of a frictionless electromagnetic force balance without removing the liquid from the system. The device included a compartmentalized container through which the UF_6-HF flowed, and the inlet and the outlet tubes, which lie in the same horizontal plane, connected to the external lines by metallic bellows. The container and its contents were supported by a pivot at the bellows and by a vertical rod passing through the container. This vertical rod and the movable member of the force-balance are parts of another lever system. Since the weight of the container was counterbalanced, only the weight of the liquid needed to be compensated by the force balance. The force balance was strictly linear; i.e., the torque that it exerted was proportional to the current supplied. A detector of any motion of the container generated a signal which, after amplification, determined the current to the force balance necessary to reestablish equilibrium. This current indicated directly the density of the liquid which was recorded on a remote panel. The performance of the densitometer was verified by measuring the density of pure UF_6 and of pure HF which are reported in Fig. 13. These measurements established that an overall precision of ± 0.6% was attainable.

2.3.1.4 Liquid Level. The level of the liquid in the sphere is a fundamental parameter for the approaches to criticality. Knowledge of the level was obtained in two different ways: 1) by determining the level in the mixing container by an ultrasonic device,

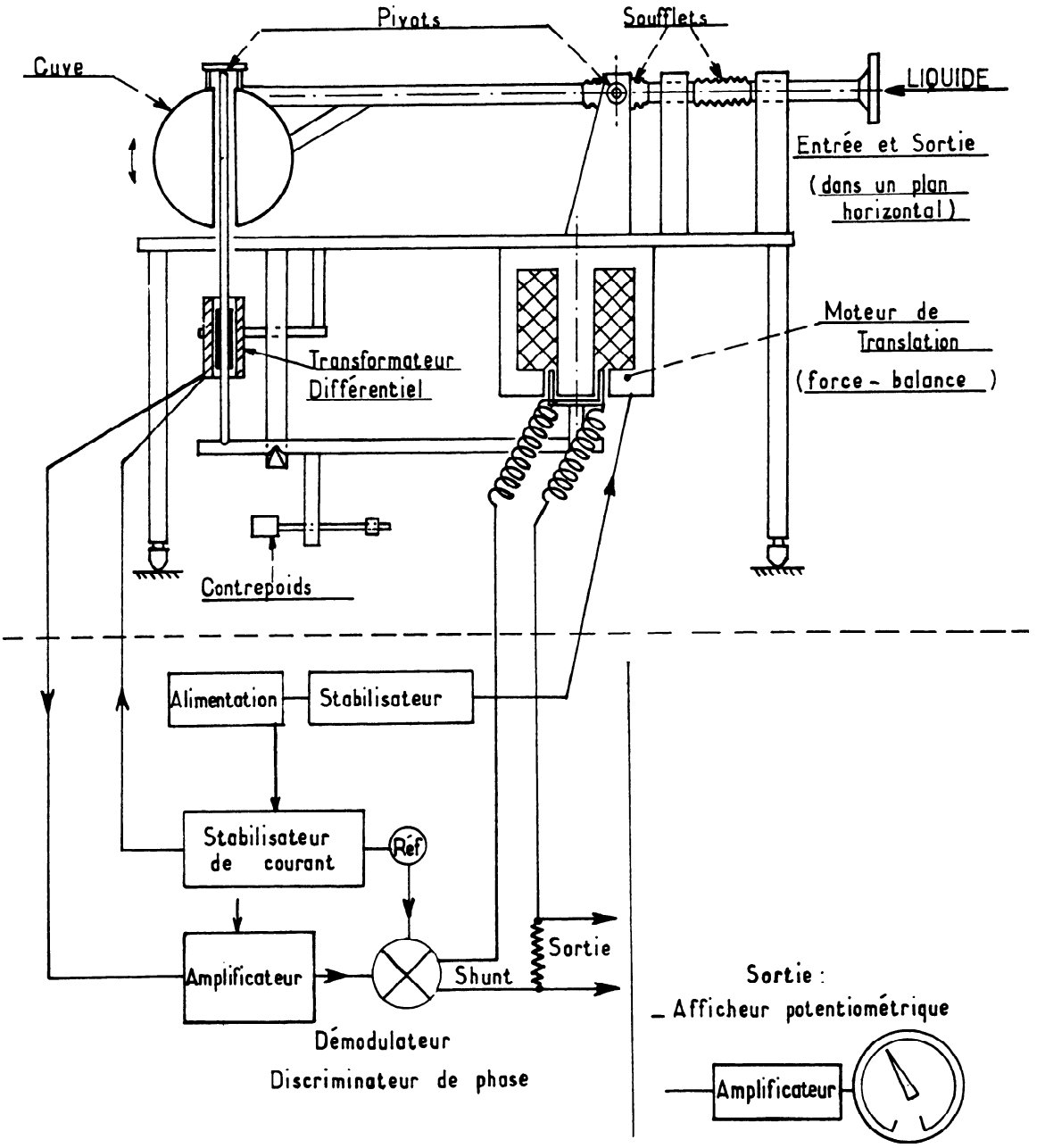

Fig. 12. Diagram of the SEAM-Type Densitometer.

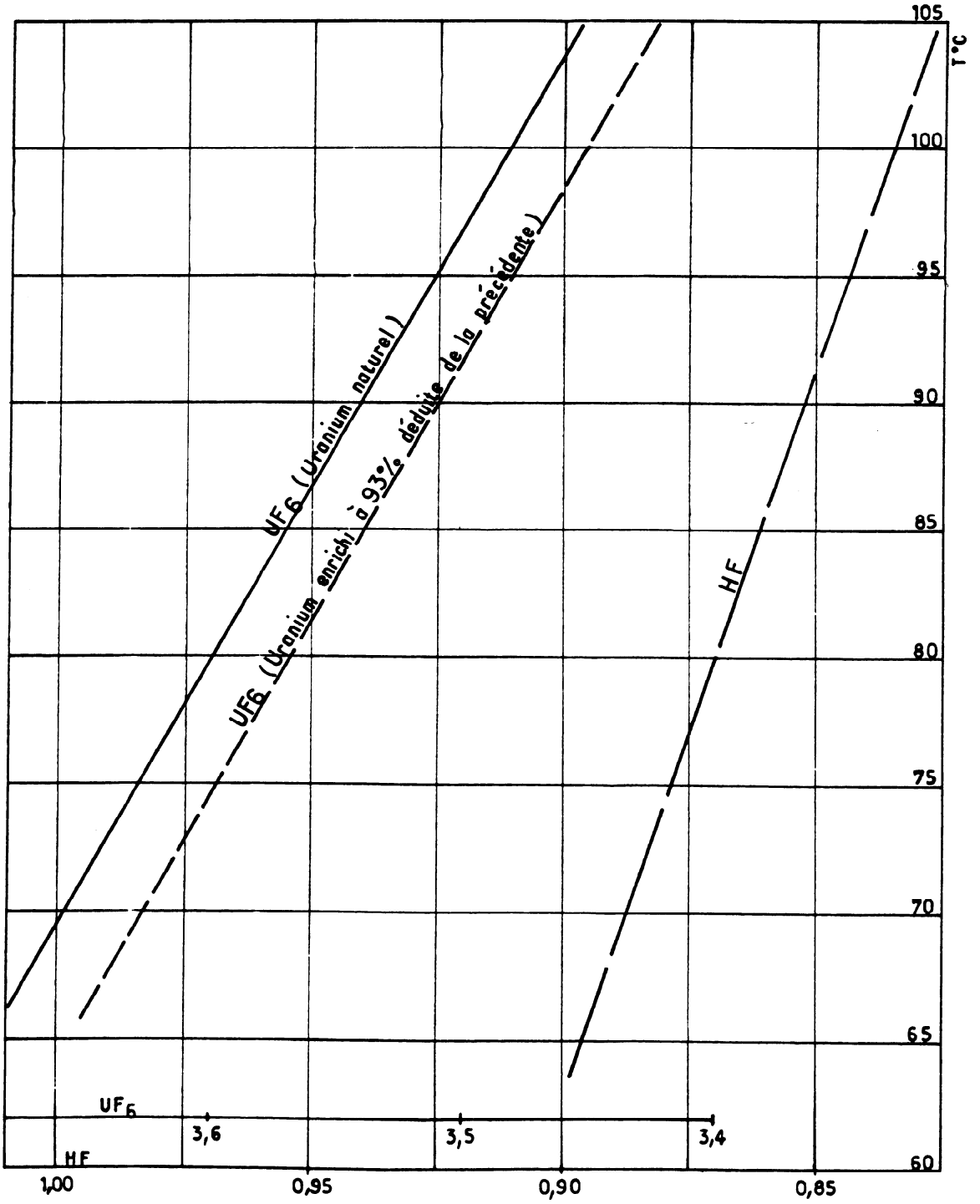

Fig. 13. Experimentally Established Curves of Density as a Function of Temperature.

an indirect measurement, and 2) by measuring the level in the sphere with a magnetic float, a direct measurement. The indirect method, although imprecise, served as a guide during the early experiments.

Approaches to criticality were controlled by the direct method of level indication to a precision of ± 0.1 mm. The instrument consisted of 6-mm-diam Monel tube mounted on the vertical diameter of the sphere serving as a guide for a freely sliding Monel float containing an internal magnet. A member, free to move vertically inside this tube, was mounted in such a manner that its motion followed that of the float. When this member was at the same level as the float, a contact, closed magnetically, controlled the remote indicator of its position. The system was calibrated for the effect of changes in density by observations with liquids of various densities.

In addition to this instrument, a second magnetic float indicated a completely filled sphere.

2.3.2 Physico-Chemical Measurements. These measurements served to determine the H:U ratio of the mixture and to verify its homogeneity. They were carried out in an analytical laboratory adjoining the experimental cell; tubing connected the laboratory directly to the sampling station for "on line" analyses. The analytical system consisted of the sampling station and its tubing, the analyzers, the control desk, and a calibration stand (a bank of standards) for the analyzers.

2.3.2.1 Samplers and Their Tubing. Sampling points were distributed throughout the system at locations appropriate to, for example, control of the purity of the materials after separation or control of the H:U ratio of the mixture during an experiment.

The Monel syringe-type samplers, designed by SRTI and illustrated in Fig. 14, consisted of a pneumatically actuated piston sliding within a pressurized stuffing box. Bellows ensured leak tightness between the compressed air region of the system and the volume filled with the UF_6-HF mixture. The sample was taken in two 2-mm-diam holes at the end of the piston and perpendicular to its axis. In its forward position, the piston was immersed in the UF_6-HF mixture and the

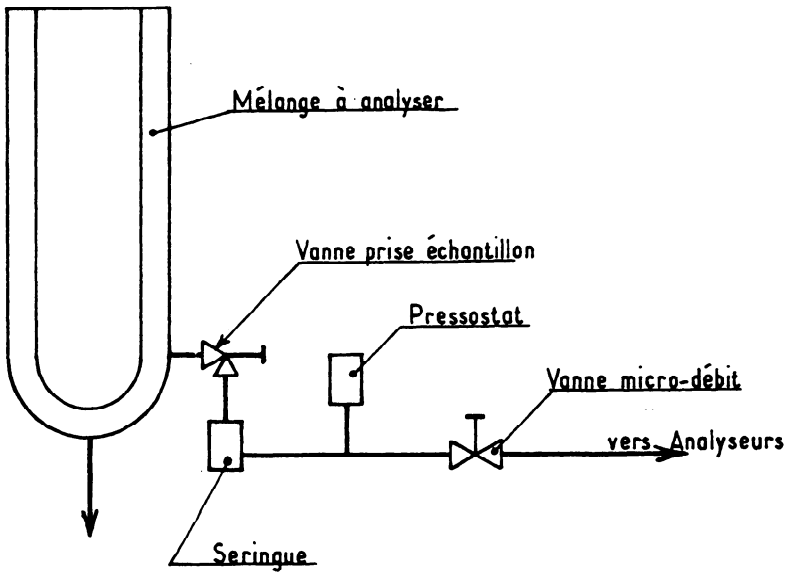

Schéma d'une ligne d'analyse

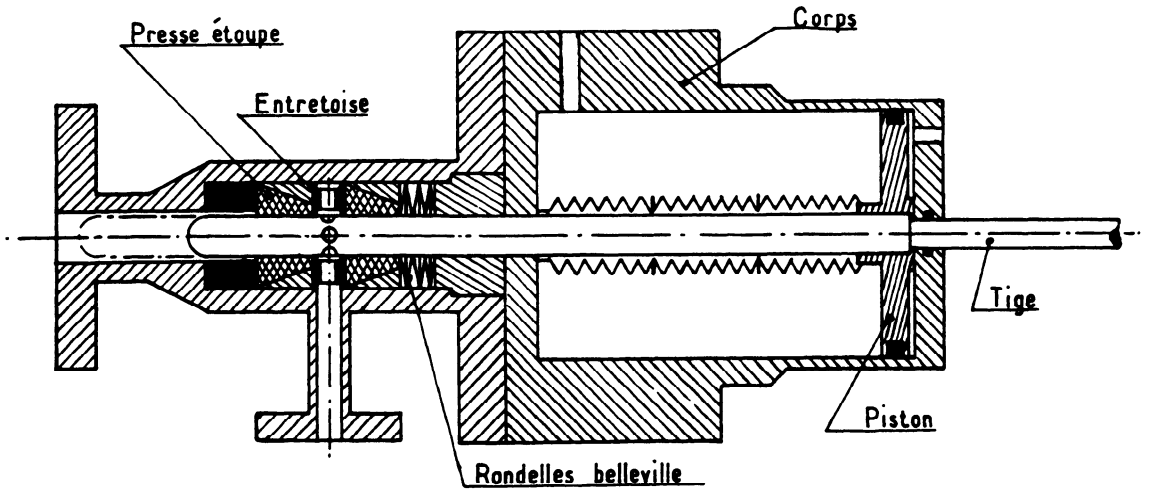

Fig. 14. Schematic Diagram of an Analysis Line and of a Syringe.

volume was filled. In its backward position, after the piston passed through the packing, the volume was connected with an expansion chamber into which the liquid was vaporized. The expansion chamber was connected with the analyzers of the laboratory through an electrically heated line.

In order that the gas passing continuously through the analyzers be maintained at constant pressure representative of the liquid mixture, a regulator at the inlet to the analyzers controlled the frequency of operation of the syringe and of the control valve located between the syringes and the analyzers.

The samplers were controlled from a central station; the gas stream could be directed toward one of the analyzers and the return stream could be directed into the cold trap to store the sample.

2.3.2.2 The Analyzers. The determination of the H:U ratio of the mixture was made by three analyzers: an infrared spectrometer, a gas-phase chromatometer, and a sonic analyzer. The overall precision of the determination by these instruments was ± 9% for H:U ratios between 5 and 25.

The analyzers were calibrated at frequent intervals by standard mixtures of natural UF_6 and HF.

2.3.3 Neutron Instrumentation. Neutron multiplication measurements during approaches to criticality were made with eight identical channels, each of which consisted of a BF_3 counter able to withstand temperatures of 120°C and located in the reflector tank, and the necessary electronic and recording equipment. The data were transmitted to a central printing unit which was able to select automatically the counting sequence.

One neutron safety channel monitored the UF_6-HF mixing and a second one monitored the actual experiments.

The low flux safety system consisted of two identical parallel channels, each including a BF_3 detector placed in the tank, a pulse preamplifier, and an ictometric period meter (a period meter using a dc charge integrator) with recorded response. Each covered the range 0.7 to 1.4 x 10^3 neutrons cm^{-2} sec^{-1}.

The high flux safety system consisted of two identical parallel channels, each including a CCS-type ionization chamber placed in the tank, a preamplifier, and a logarithmic period meter with recorded response; this system covered an overall range between 6 and 6×10^8 neutrons cm^{-2} sec^{-1}; the desired portion of this range was obtained by changing the location of the detector.

The safety system initiated two methods of shutdown: the fast shutdown resulted from releasing the safety skirt which introduced a negative reactivity of 1700×10^{-5} in 0.8 sec; the slow shutdown resulted from draining the sphere through two pneumatically controlled, normally open, 50-mm-diam valves, in parallel.

2.3.4 Health Physics Instrumentation. Gamma radiation and surface contamination by alpha particles were monitored in the area where the experiment was performed and in the areas where the UF_6 and HF were handled, processed, and stored.

2.4. Nuclear Criticality Safety and Personnel Protection

2.4.1 Nuclear Criticality Safety. The UF_6 and its mixtures with HF were stored, transferred, and mixed in equipment of favorable geometry, using either cylinders or annular cylinders that provided safety. In addition, the mixing container was monitored for neutron multiplication.

2.4.2 Personnel Protection.

Protection Against Radiation: As mentioned above, all experiments were remotely operated from the control room.

Protection Against Contamination: The atmosphere of the caisson enclosing the experimental system was continuously monitored.

Protection Against Chemical Agents: Personnel were provided with protective clothing and safety equipment for use when handling hydrofluoric acid, chlorine trifluoride, and uranium hexafluoride.

3. EXPERIMENT PROCEDURE AND TECHNIQUES

3.1. Sequence

3.1.1 Preparation of the Mixture. In order to make successive approaches to criticality in the sphere, the following preliminary steps were carried out in the preparation of a mixture with a given H:U ratio:

1. Calculate the quantities of UF_6 and of HF necessary to prepare the volume of liquid required to fill the sphere, the densitometer, the connecting piping, and the bottom of the mixing container (see Fig. 8);
2. Heat the UF_6 and HF containers;
3. Allow the UF_6, heated to about 78°C in its storage container, to flow into the top of the mixing container. The amount transferred was determined from the continuously weighed UF_6 storage container. The precision of this weighing was ± 1 kg.
4. After the UF_6 had been transferred, allow the HF to flow into the bottom of the mixing container. The resulting bubbling homogenized the mixture. The amount transferred was determined from the continuously weighed HF container. The precision of this weighing was ± 0.3 kg. In some instances, the required quantity of HF exceeded the capacity, 22 kg, of the weighing container, necessitating several incremental additions. The temperature of the HF in each of the partial transfers was greater than the temperature at which separation of the components of the liquid mixture at the concentration under study occurred.
5. Start a vibrator in the mixing container to homogenize the mixture as soon as the transfer of HF began. The temperature during the mixing was controlled at a value appropriate to the operation.
6. Obtain and analyze one sample from the vapor phase and one from the liquid phase after two to four hours of homogenization, when the temperature of the mixture was well stabilized at the desired level. The critical experiment was not begun until the analytical results had been received from the laboratory and the desired concentration, temperature, and pressure had been verified on the binary UF_6-HF phase diagram.

3.1.2 Approach to Criticality. The liquid flowed by gravity into the sphere through a pneumatically controlled valve, a filter to retain any solid particles present in the mixture, the densitometer, and a remotely controlled microflow valve, all shown in Fig. 8.

The first phase of an experiment consisted of filling the ~10 ℓ volume between the mixing container and the sphere in order to obtain a value of the density of the mixture. Knowing this density, the level-indicating instrument described in Section 2.3.1.4 was calibrated. A third sample, taken from the flow line, permitted verification of the previously determined composition of the mixture. At the same time, the neutron counting channels were put in service to determine the background.

The second phase of an experiment consisted of the actual approach to criticality. The spherical segment originally installed for control was not used during any of the experiments and remained in its completely withdrawn position. In each case, a reciprocal neutron multiplication curve was plotted as a function of the volume of liquid in the sphere. This volume was obtained from the reading of the level indicator and from the volume calibration curve of each sphere.

These multiplication curves were based on a large number of points, each derived from a series of neutron counts and measurements of the density, the pressure, the temperature, and the liquid level. The homogeneity of the mixture was monitored continuously throughout an experiment by density measurements of the inflow with the SEAM-type densitometer and by controlling temperature and pressure of the mixture in the sphere and temperature of the water reflector (the constancy of these parameters shows homogeneity of the mixture).

3.1.3 Termination. An experiment was concluded when extrapolations showed a critical level in the sphere or the filled sphere was subcritical. At this time the drain valves were opened, allowing the mixture to flow into the drain tank preparatory to separation for the next experiment.

3.2. Auxiliary Operations.

The principal auxiliary operations necessary to preparations for the actual experiments included evaluation of the performance of the systems, fractional crystallization, purification of components by distillation, calibration of the measuring instruments, pretreatment of the system and regeneration by chlorine trifluoride, dehydration of HF by gaseous fluorine, determination of the leak tightness of the system by means of a helium spectrometer, replacement of the spheres, and maintenance of fittings such as valves, etc.

3.3. Problems Encountered

The experiments imposed a considerable amount of work on the operating personnel. They had to perform a great variety of operations with hazardous materials such as UF_6-HF mixtures and ClF_3. When the apparatus operated normally, preparation for each experiment required an average of two weeks; the average duration of an experiment was 15 hours.

Several incidents occurred during the experiments, with no consequence to operators. Typical incidents were leaks of UF_6 or of a UF_6-HF mixture into the cell atmosphere, resulting from a break in a valve bellows, corrosion of a joint, etc. The complexity of the apparatus made decontamination very tedious and time-consuming. Disassembly and replacement of faulty equipment, which required subsequent fluorination and leak tightness testing, necessitated frequent operations while wearing special protective clothing and self-contained breathing apparatus as precautionary measures and caused costly loss of time.

4. RESULTS

4.1. Experimental

4.1.1 Quantities Measured.

4.1.1.1 Density. The curves presented in Fig. 4 were established during the preliminary experiments and show the density of the liquid UF_6-HF mixtures as a function of the temperature and of the composition expressed as the H:U ratio. These results were obtained with natural uranium by the method described in Section 2.3.1.3. Tables 1 and 2 and the curves of Figs. 15 and 16 show, respectively, the density of the UF_6-HF mixtures, in which the uranium was enriched to 93% in ^{235}U, and the concentration of total uranium (see also Fig. 17) as a function of the H:U ratio. These values are known with a precision between 0.5 and 0.7%.

The tests of the densitometer established that its precision was 0.6%.

4.1.1.2 Temperature and Pressure. The error associated with the temperature measurement of each experiment was ± 0.3°C.

The pressure was measured with a precision of ± 0.3%. The measurement revealed a marked difference between the pressure in the gas phase of the UF_6-HF mixture and the theoretical value derived from the liquid-vapor equilibrium phase diagram of the binary mixture shown in Fig. 3. This difference may possibly be due to the presence of gas, such as traces of nitrogen, dissolved in the UF_6 and more probably to fluorine in the HF. These gases were used for auxiliary operations, such as nitrogen for purging the system and fluorine for dehydrating the HF.

4.1.1.3 Composition of the Mixture. The composition of the mixture was determined in two steps. Before each experiment, the analytical laboratory determined the H:U ratio as described in Section 2.3.2. This value was then confirmed from the curves of Fig. 15 and the measured temperature and density. This procedure made it possible to determine the H:U ratio with high precision and to obtain consistent values in each experiment.

Table 1. Density of UF_6-HF Mixtures in Which the Uranium Was Enriched to 93% in ^{235}U. The values are expressed in g/cm^3.

H:U	70°C	75°C	80°C	90°C	100°C	110°C
0	3.626	3.597	3.567	3.510	3.451	3.394
1	3.062	3.031	3.000	2.938	2.876	2.814
2	2.727	2.693	2.660	2.595	2.528	2.463
3	2.462	2.432	2.402	2.343	2.283	2.224
4	2.247	2.221	2.195	2.142	2.089	2.037
5	2.091	2.065	2.039	1.988	1.936	1.884
6	1.985	1.960	1.935	1.884	1.833	1.783
7	1.909	1.885	1.860	1.810	1.760	1.711
8	1.846	1.821	1.797	1.749	1.700	1.651
9	1.784	1.760	1.736	1.688	1.641	1.593
10	1.723	1.700	1.676	1.629	1.582	1.536
11	1.664	1.641	1.619	1.573	1.527	1.481
12	1.612	1.589	1.566	1.520	1.474	1.429
13	1.565	1.543	1.521	1.476	1.431	1.386
14	1.527	1.505	1.482	1.438	1.393	1.350
15	1.492	1.470	1.448	1.406	1.362	1.319
16	1.460	1.439	1.418	1.376	1.333	1.291
17	1.432	1.411	1.390	1.349	1.307	1.267
18	1.405	1.384	1.364	1.324	1.284	1.244
19	1.380	1.360	1.340	1.302	1.262	1.223
20	1.358	1.339	1.319	1.281	1.242	1.204
21	1.337	1.318	1.299	1.262	1.224	1.187
22	1.318	1.299	1.281	1.245	1.208	1.173
23	1.301	1.283	1.265	1.230	1.195	1.160
24	1.286	1.269	1.252	1.218	1.183	1.149
25	1.273	1.256	1.240	1.207	1.173	1.141
26	1.262	1.245	1.229	1.197	1.164	1.133
∞	0.886	0.877	0.869	0.852	0.835	0.818

Table 2. Uranium Concentration in a Mixture of UF_6 and HF in Which the Uranium Was Enriched to 93% in ^{235}U. The values are expressed in g/cm^3.

H:U	70°C	75°C	80°C	90°C	100°C	110°C
0	2.434	2.415	2.395	2.357	2.317	2.279
1	1.945	1.925	1.905	1.866	1.827	1.787
2	1.643	1.623	1.603	1.564	1.523	1.484
3	1.411	1.394	1.377	1.343	1.309	1.275
4	1.228	1.214	1.200	1.171	1.142	1.113
5	1.092	1.078	1.065	1.038	1.011	0.984
6	0.993	0.980	0.968	0.942	0.917	0.892
7	0.916	0.904	0.892	0.868	0.844	0.821
8	0.851	0.839	0.828	0.806	0.783	0.761
9	0.791	0.780	0.770	0.748	0.728	0.706
10	0.736	0.726	0.716	0.696	0.676	0.656
11	0.686	0.677	0.668	0.649	0.630	0.611
12	0.642	0.633	0.624	0.605	0.587	0.569
13	0.603	0.594	0.586	0.569	0.551	0.534
14	0.570	0.561	0.553	0.536	0.520	0.504
15	0.539	0.531	0.523	0.508	0.492	0.477
16	0.512	0.505	0.497	0.483	0.467	0.453
17	0.488	0.481	0.473	0.459	0.445	0.432
18	0.465	0.458	0.451	0.438	0.425	0.412
19	0.444	0.438	0.431	0.419	0.406	0.394
20	0.425	0.421	0.413	0.401	0.389	0.377
21	0.408	0.402	0.396	0.385	0.374	0.362
22	0.392	0.386	0.381	0.370	0.359	0.349
23	0.377	0.372	0.367	0.357	0.347	0.337
24	0.364	0.359	0.354	0.345	0.335	0.325
25	0.352	0.347	0.343	0.334	0.324	0.315
26	0.341	0.336	0.332	0.323	0.314	0.306
∞	0.000	0.000	0.000	0.000	0.000	0.000

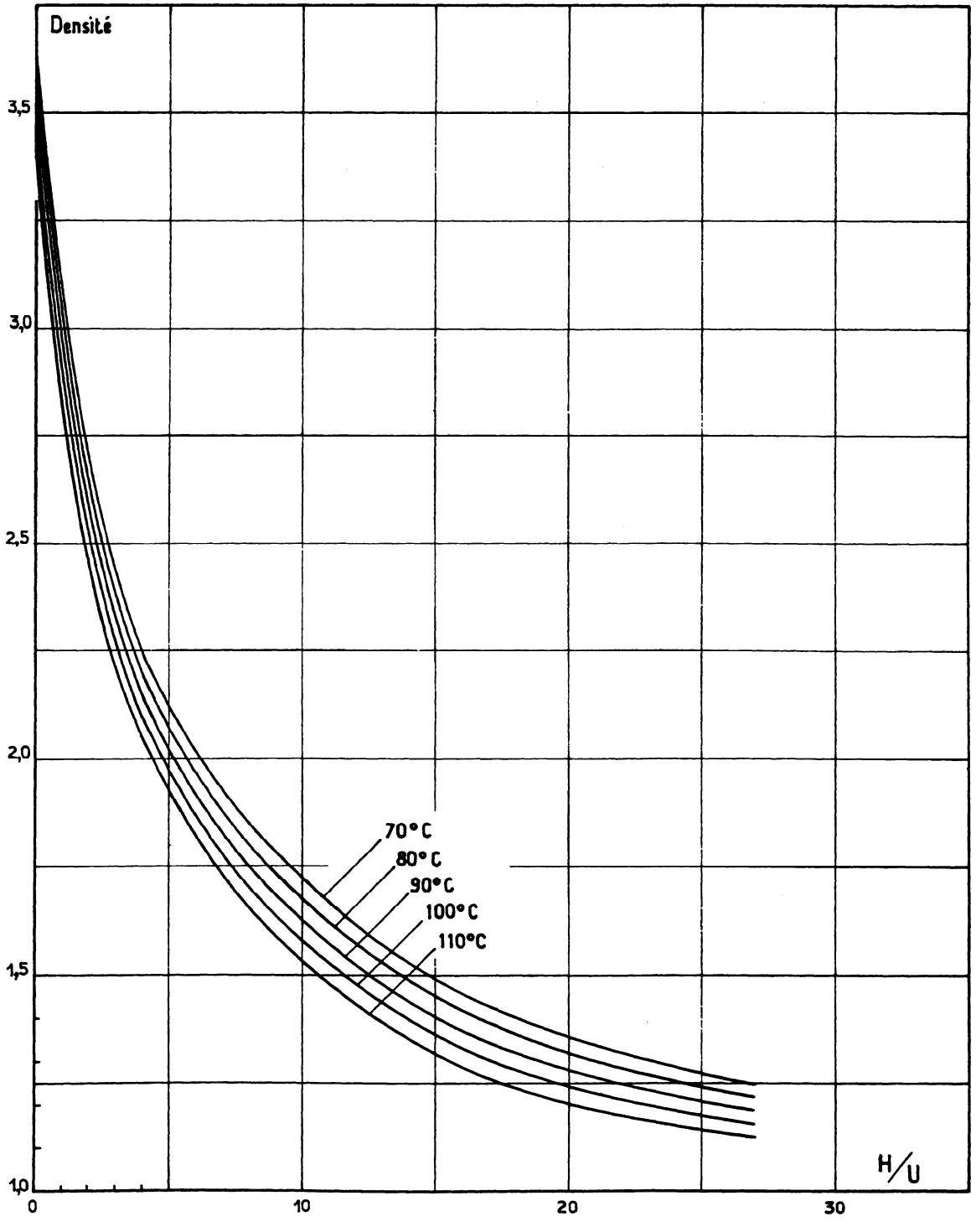

Fig. 15. Density of UF_6-HF Mixtures as a Function of the H:U Ratio.

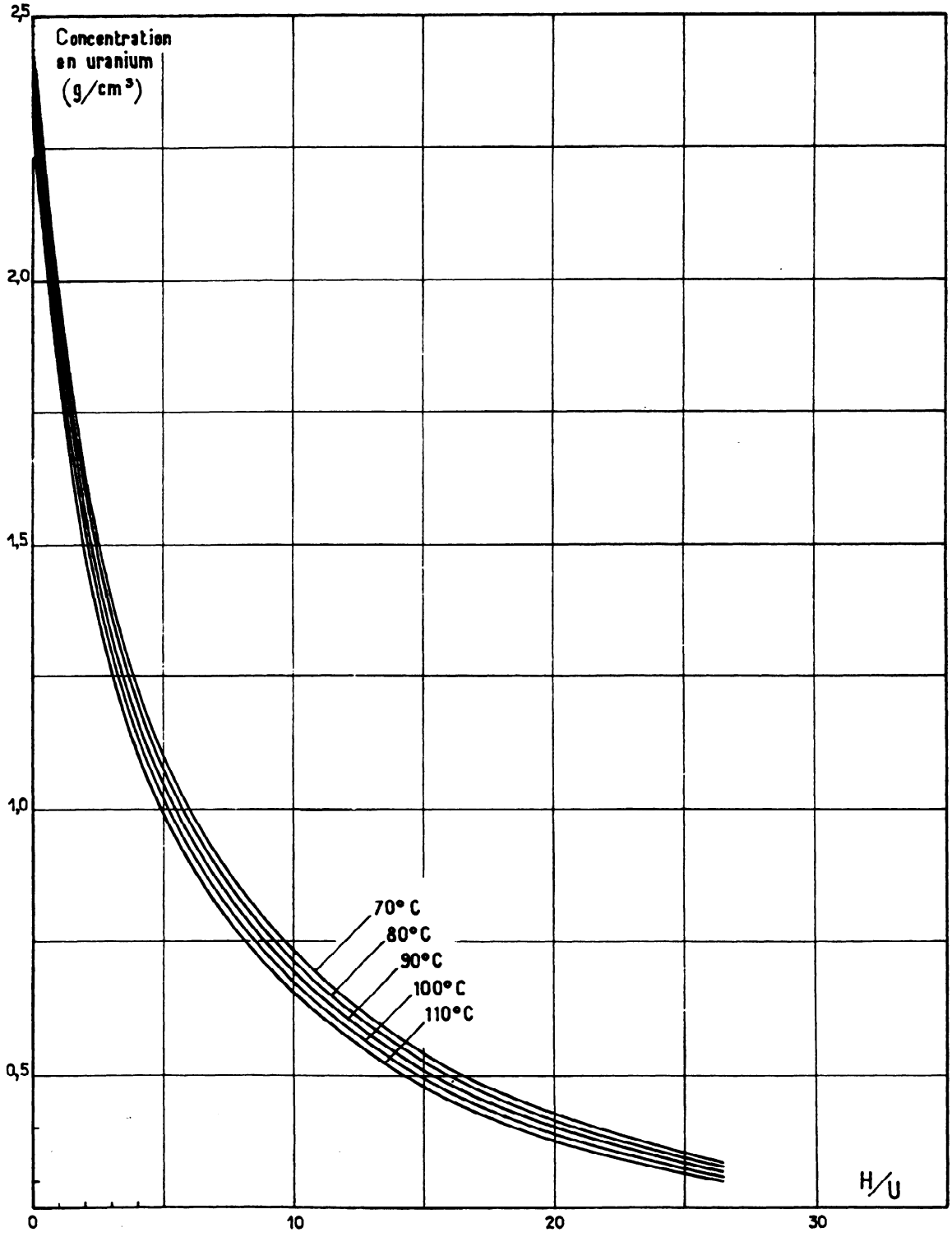

Fig. 16. Concentration of Uranium in Mixtures of UF_6-HF in Which the Uranium was Enriched to 93% in ^{235}U.

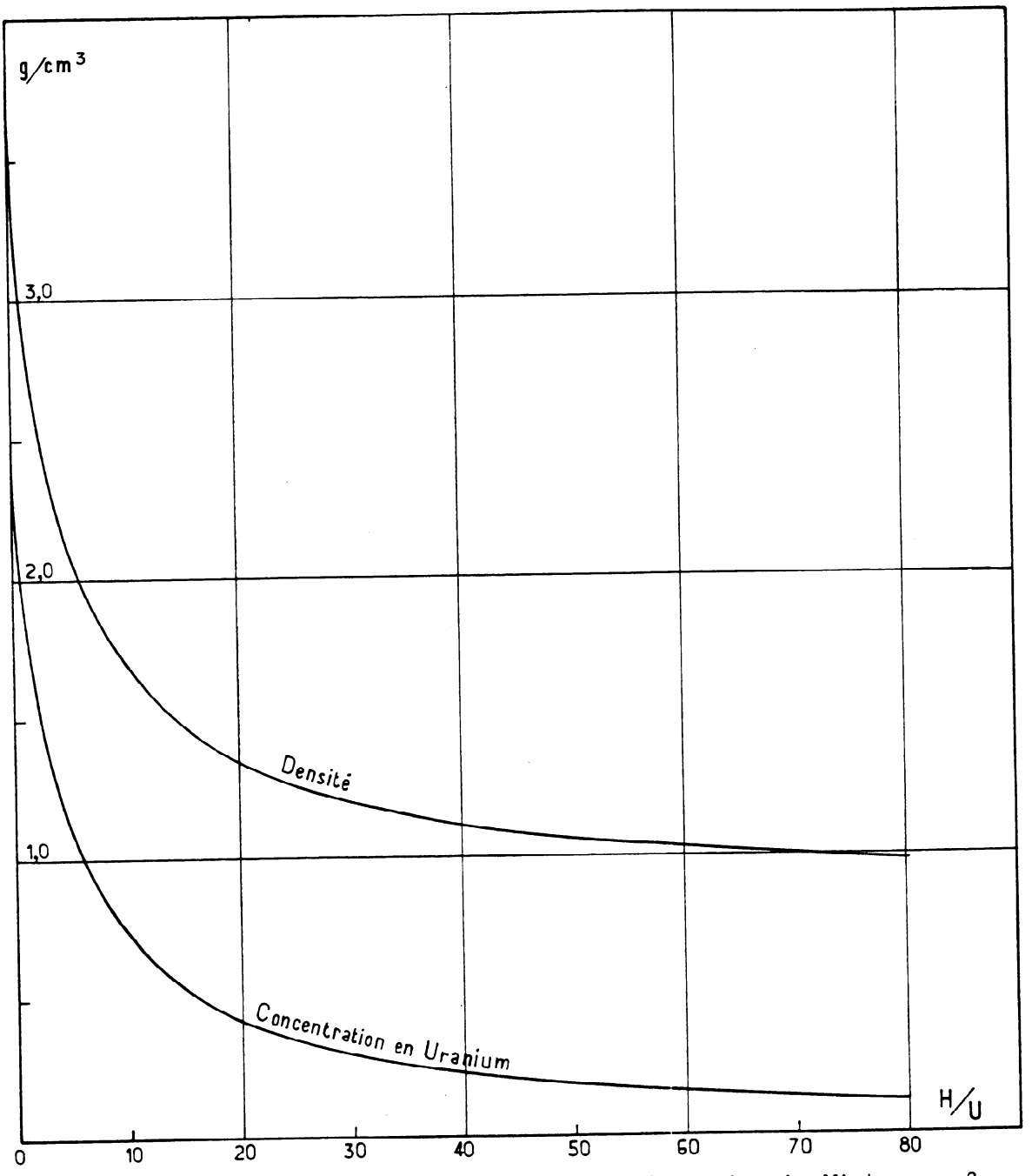

Fig. 17. Density and Concentration of Uranium in Mixtures of UF_6-HF at 75°C as a Function of H:U. The uranium was enriched to 93% in ^{235}U.

4.1.2 Data. The 150 kg of UF_6 available was found to be insufficient to determine the critical conditions for pure UF_6. The 400- and the 450-mm-diam spheres were found to be subcritical for all concentrations studied; they were used in tests checking the instrumentation and the control of the experimental equipment and they indicated the final choice of the 510- and the 540-mm-diam spherical containers for the subsequent experiments.

The experiments with these latter spheres completely covered the range of concentrations finally selected for the study. Depending on the experimental conditions and the composition of the mixture, criticality was approached very closely in certain experiments, to within 0.5 ℓ of the critical volume; in most of the others the critical volume could be reliably extrapolated from the neutron multiplication curves. Criticality was achieved in the 540-mm sphere at an H:U of 16.9 as described in Table 3.

When the filled sphere would have been supercritical, the critical volume, which is the value given as an experimental result in Table 3, was that of a truncated sphere.

When the filled sphere was subcritical, the critical volume reported in the table of experimental results was obtained from a linear extrapolation of the neutron multiplication curves. This procedure is illustrated in Fig. 18.

The capacities of both the 510- and the 540-mm-diam spheres, which were constructed of 4-mm-thick Monel 400, were precisely determined by calibration; the mean diameters were calculated from these experimental values. The results were:

510-mm-diam sphere

Capacity:	69.03 ± 0.03 ℓ
Mean Inside Diameter:	508.96 ± 0.06 mm

540-mm-diam sphere

Capacity:	82.07 ± 0.04 ℓ
Mean Inside Diameter:	539.17 ± 0.08 mm .

The experimental data are given in Table 3.

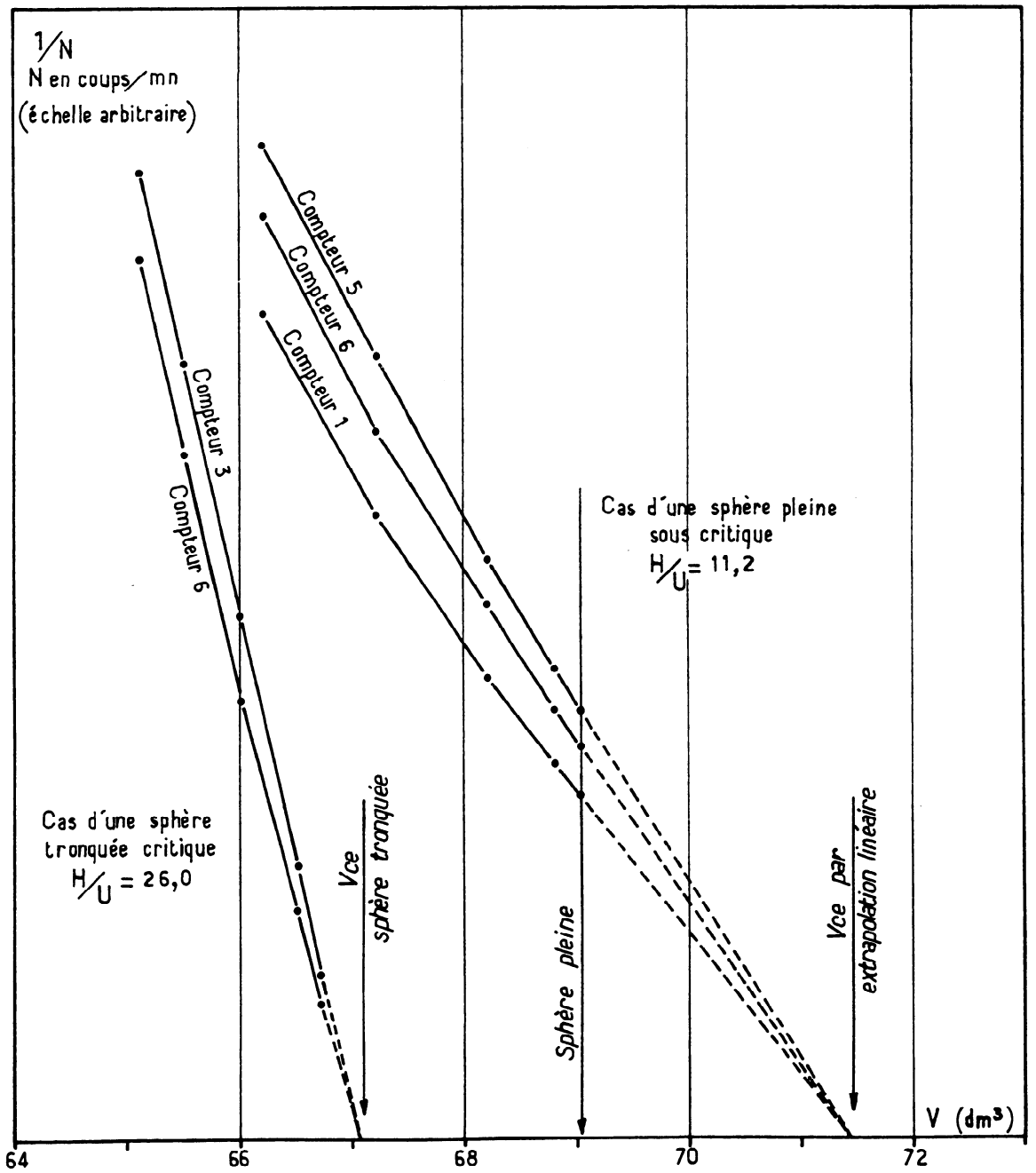

Fig. 18. Examples of Approaches to Criticality in the 510-mm-diam Sphere.

Table 3. Experimental Results.

	Nominal Diameter of Spherical Container (mm)											
	400	540	540	510	510	510	540	510	510	510	510	540
H:U	0	5.7	9.9	10.8	11.2	15.2	16.9	21.0	26.0	38	74	82
Δ^a (H:U)		0.1	0.2	0.2	0.2	0.3	0.3	0.4	0.7	1	2	3
T (°C)	77	89.0	75.0	85.8	75.1	74.8	94.3	74.3	75.0	75.6	75.1	75.3
ΔT (°C)	0.3	0.3	0.3	0.3	0.3	0.3	0.3	0.3	0.3	0.3	0.3	0.3
ρ (UF_6-HF) (g/cm^3)	3.58	1.92	1.71	1.61	1.63	1.467	1.336	1.321	1.245	1.149	0.990	0.973
$\Delta\rho$ (g/cm^3)	0.02	0.02	0.01	0.01	0.01	0.009	0.008	0.880	0.007	0.007	0.006	0.006
Liquid Height in the Sphere (mm)	Full	Full	472.7	Full	Full	Full	509.6	465.8	461.7	461.0	Full	461.2
Critical Volume V_c (ℓ)		85.0	78.5	76.0	71.3	69.4	81.3	67.3	67.1	67.0	71.3	77.2
ΔV_c (ℓ)		0.4	0.2	0.7	0.5	0.2	0.2	0.2	0.2	0.2	0.3	0.2

a. The values designated by Δ represent uncertainties in the corresponding quantities.

4.2. Interpretation of Results and Correlation with Theory.

4.2.1 Transformation of Reactivity to an Ideal Sphere. The differences between an ideal sphere and an experimental sphere, apparent from examination of Fig. 9a, are the guide tube of the level-measuring float, the lack of absolute sphericity, and the upper and lower connections.

The 6-mm-i.d. Monel guide tube of the level-measuring float had 1-mm-thick walls and displaced about 250 cm^3 of liquid. The capacity of the sphere was determined with the tube and the float in position. Although the tube was a thermal neutron absorber, its effect on reactivity was neglected because the thermal neutron flux on the axis of the sphere was small.

It was estimated that the lack of sphericity of an experimental sphere was sufficiently slight to cause negligible reactivity differences with respect to an ideal sphere of the same capacity.

The negative reactivity introduced into the experiment by the Monel wall is calculated in Section 5.1 as 1190 x 10^{-5} per mm thickness. If the effective neutron multiplication factor k_{eff} is proportional to the spherical surface, the reactivity due to the absence of this metal at the two openings may be expressed as

$$\Delta k_{eff_1} = \frac{[k_{eff}(0 \text{ mm}) - k_{eff}(4 \text{ mm})] \times (s_1 + s_2)}{S}$$

where

s_1 = the area of the bottom opening ($\simeq$ 15 cm^2)

s_2 = the area of the upper opening ($\simeq$ 31 cm^2)

S = the external surface area of the sphere ($\simeq$ 8137 cm^2 for a 510-mm-diam sphere)

$$\Delta k_{eff_1} \simeq + 27 \times 10^{-5} \quad .$$

The surface of the upper opening, however, was not completely water-reflected and this "void" resulted in a negative reactivity. For a sphere 510 mm in diameter and at an H:U of 17, it was found by DSN calculations that

$$k_{eff_{reflected}} - k_{eff_{unreflected}} \simeq 0.28 .$$

If k_{eff} is proportional to the area of the reflecting surface, the negative reactivity due to the lack of total water reflection at the upper opening was

$$\Delta k_{eff_2} \simeq - 106 \times 10^{-5} .$$

The mixture was introduced into the sphere through a 42.7-mm-i.d. pipe about 400 mm long connected to the bottom of the sphere. The reactivity due to the mixture occupying this connection was definitely less than it would have been were the same volume uniformly distributed over the surface of the sphere. The reactivity, Δk_{eff}, attributable to an increase of 1 mm in the diameter of the sphere is 125×10^{-5} as shown in Section 4.2.2.1.3. Therefore the increase in reactivity due to increasing the diameter 1.4 mm is

$$\Delta k_{eff_3} < 175 \times 10^{-5} .$$

Although these evaluations are only approximate, it is possible to state that the difference in reactivity of an ideal sphere and that of an experimental sphere of the same volume is very slight.

4.2.2 Extrapolation of Experimental Data to a Critical Ideal Sphere. The experimental data in Table 3 may be divided into two groups: (1) those describing a subcritical full sphere and (2) those describing a critical truncated sphere. It is now necessary to establish methods of extrapolation to obtain the critical diameters of ideal spheres.

4.2.2.1 Extrapolation from a Subcritical Sphere

4.2.2.1.1 Neutron Counter Response. The relation between the total number of neutrons produced per unit time in the core and the strength of the auxiliary neutron source is

$$N = \frac{S}{1 - k_{eff}}$$

where

N = the total number of neutrons produced per second in the core

S = the strength of the auxiliary source, in neutrons per second

k_{eff} = the effective neutron multiplication factor.

Consider a homogeneous, spherical, subcritical core and a BF_3 counter placed in the reflector. The total number of neutrons that leak from the surface of the sphere per unit time, Nf, is proportional to N in a stable subcritical system.

In the case of spherical symmetry, the leakage flux is uniform and isotropic; thus the counter always captures the same fraction of the leakage neutrons. The response of a BF_3 counter is proportional to the number of neutrons captured:

$$\mathcal{N} = \alpha N$$

where

$\mathcal{N}$ = the counter response in counts per unit time

α = a coefficient depending specifically on the counter and on the relative positions of the counter and the core,

and

$$\mathcal{N} = \alpha \frac{S}{1 - k_{eff}} . \qquad (2)$$

4.2.2.1.2 Determination of k_{eff}. The auxiliary source of neutrons in a UF_6-HF medium is the spontaneous fissions and the (α,n) reaction in fluorine. This source is

$$S = s\ V$$

where

s = the specific neutron source strength

V = the volume of the fissile material in the sphere.

Equation (2) becomes

$$\mathcal{N} = \frac{s\ \alpha\ V}{1 - k_{eff}}$$

and

$$k_{eff} = \frac{\mathcal{N} - s\ \alpha\ V}{\mathcal{N}} \quad . \tag{3}$$

In the experiment $\mathcal{N}$ and V were measured. The value of $s\alpha$, necessary to calculate k_{eff}, was determined as follows: the count rates were measured following successive incremental additions of the mixture to the sphere and are plotted in Fig. 19 as a function of the volume of the mixture in the sphere. For small volumes where the neutron multiplication is negligible, the curve is linear and has a slope equal to $s\alpha'$, which may be determined graphically.

The coefficients α' and α depend on the counter and on the relative counter-source position. However, this relative position changes as the sphere is filled. The neutrons from a full sphere appear to originate at a point source located at the center of the sphere. Let d be the distance between the center of the sphere and the axis of the counter, whose plane of symmetry contains the vertical axis of the sphere. As the filling of the sphere is begun, the source may be considered as a point placed at the lower pole of the sphere; we shall designate by d' the distance between this pole and the axis of the counter.

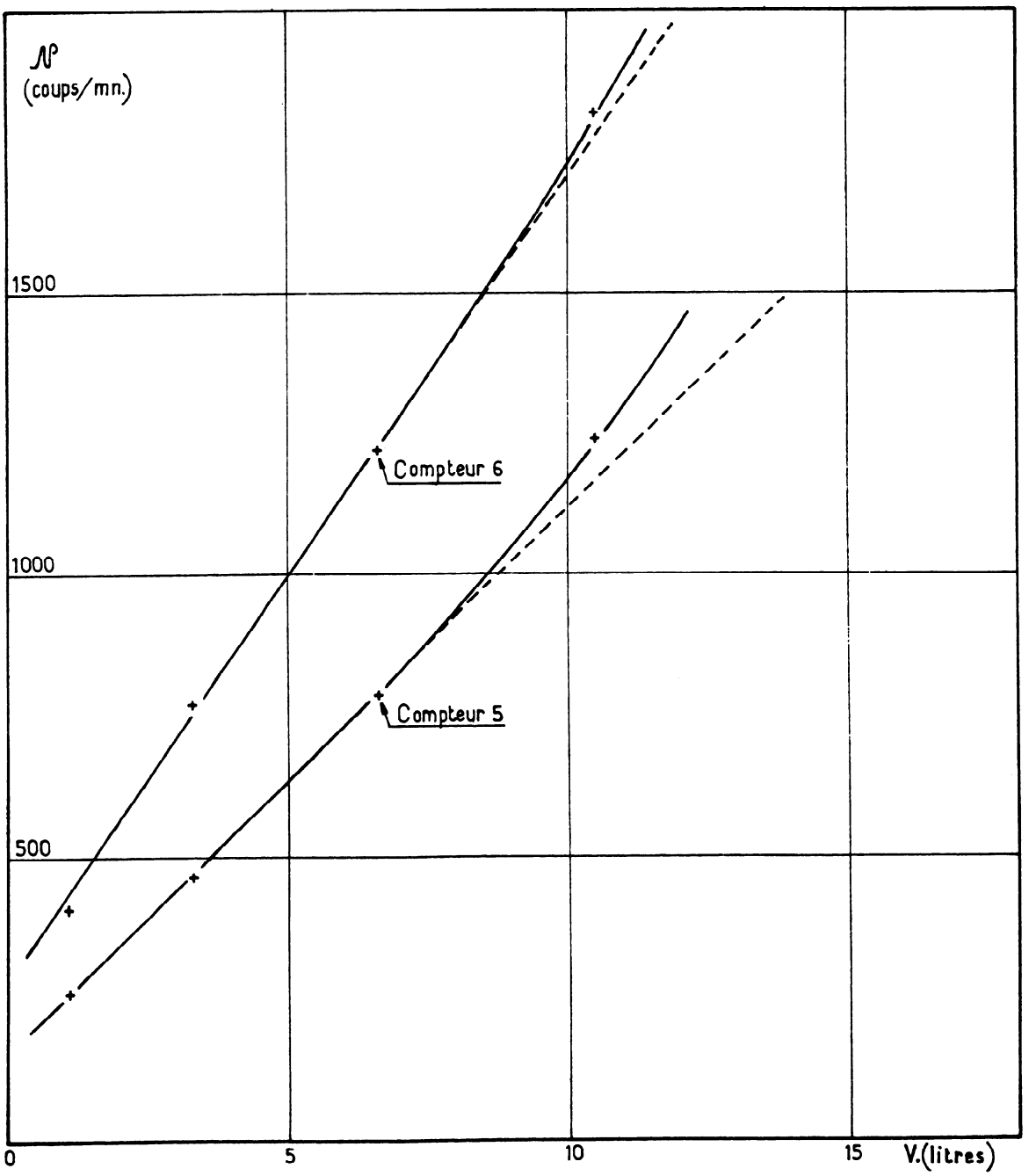

Fig. 19. An Example of the Graphical Determination of α's at an H:U of 15.2.

Assuming that the response of the counter is proportional to the geometric solid angle defined by the assumed point source and the effective volume of the counter, the following relation holds:

$$\alpha = \alpha' \left(\frac{d'}{d}\right)^2 .$$

Equation (3) is then written as

$$k_{eff} = \frac{\mathcal{N} - s\alpha' V \left(\frac{d'}{d}\right)^2}{\mathcal{N}} . \qquad (4)$$

This assumption seems reasonable if the neutron paths in the water are of the same order.

These assumptions greatly simplify the situation. However, in order to be strictly correct, one should take into account the true configuration of the source as filling of the sphere is begun rather than considering it a point source; in addition, the effects of neutron absorption in the uranium-bearing region and the diffusion and absorption of neutrons in the reflector water should be considered.

4.2.2.1.3 Variation of k_{eff} with Sphere Diameter.

Consider an ideal spherical container with a 4-mm-thick Monel wall, reflected by 30 cm of water, and filled with a mixture of UF_6 and HF. The variations in k_{eff} as a function of the inside diameter of the container, Di, for H:U ratios of 0 and 20, calculated by the DSN code in Section 5.1, are shown in Fig. 20. k_{eff} is essentially a linear function of the diameter in the region ± 20 mm about the critical diameter; in addition, the straight lines obtained for the two H:U ratios are parallel. Therefore,

$$\frac{\Delta k_{eff}}{\Delta Di} = \text{constant} \simeq 125 \times 10^{-5} \text{ mm}^{-1}$$

since $\Delta k_{eff}/\Delta Di$ is independent of the H:U ratio in the range considered.

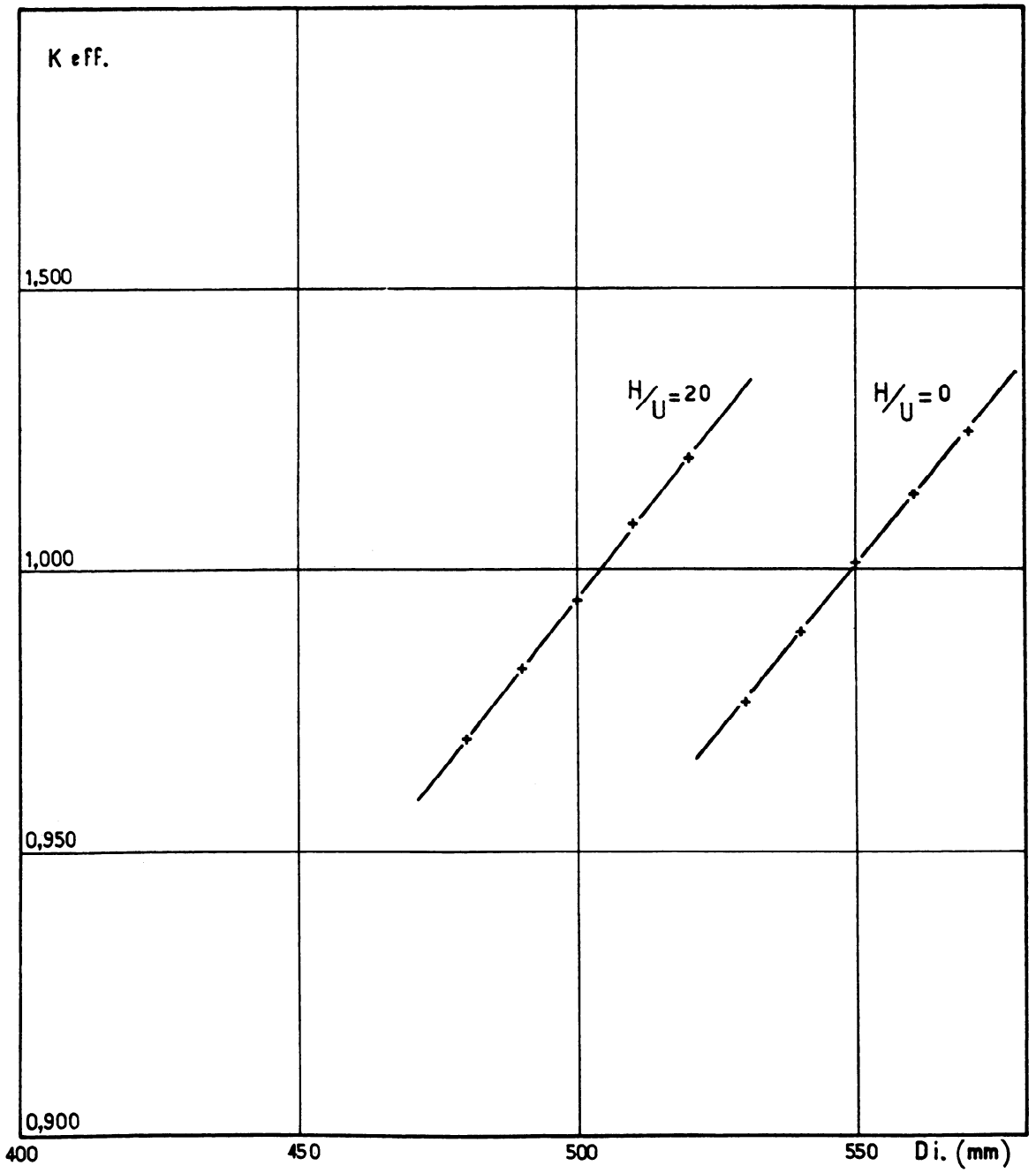

Fig. 20. Variation of the Effective Multiplication Factor as a Function of Sphere Diameter.

4.2.2.1.4 Example. The Monel sphere having an internal diameter of 508.96 mm and a capacity of 69.08 ℓ was subcritical when filled with a mixture having H:U = 15.2 at a temperature of 74.8°C.

Counters 5 and 6 were placed in symmetrical positions with respect to a vertical central plane of the sphere as shown in Fig. 21. Figure 19 shows the count rates as a function of the volume during the early stages of filling. The slope of the linear portion of the curve for Counter 5 is

$$s\alpha' = 96.0 \frac{\text{counts}}{\ell \text{ min}} .$$

The value of $\left(\frac{d'}{d}\right)^2$ was $\frac{1}{5.3}$ and of $\mathcal{N}$, for a filled sphere, was 863,144 counts/min. Equation (4) yields $k_{eff} = 0.9985$.

Similarly for Counter 6, $s\alpha' = 144 \frac{\text{counts}}{\ell \text{ min}}$, $\mathcal{N}$ = 1,459,378 counts/min, and $k_{eff} = 0.9987$. The mean value of k_{eff} is 0.9986, and

$$1 - k_{eff} = 14 \times 10^{-4}.$$

According to Section 4.2.2.1.3,

$$\Delta Di = \frac{14 \times 10^{-4}}{125 \times 10^{-5}} = 1.12 \text{ mm},$$

and the extrapolated critical diameter is

$$D_c = Di + \Delta Di = 510.08 \text{ mm},$$

corresponding to a critical volume of 69.49 ℓ.

4.2.2.2 Extrapolation from a Critical Truncated Sphere. Monte Carlo calculations were carried out for three volumes of liquid:

a. a truncated sphere with D = 540 mm, height[a] H = $\frac{3}{4}$ D and volume V

---

[a]The relatively small height of 3/4 D was chosen to ensure that differences in reactivity would not be obscured by the statistical errors inherent in the Monte Carlo method, which is the only method by which the geometry of a truncated sphere can be completely described.

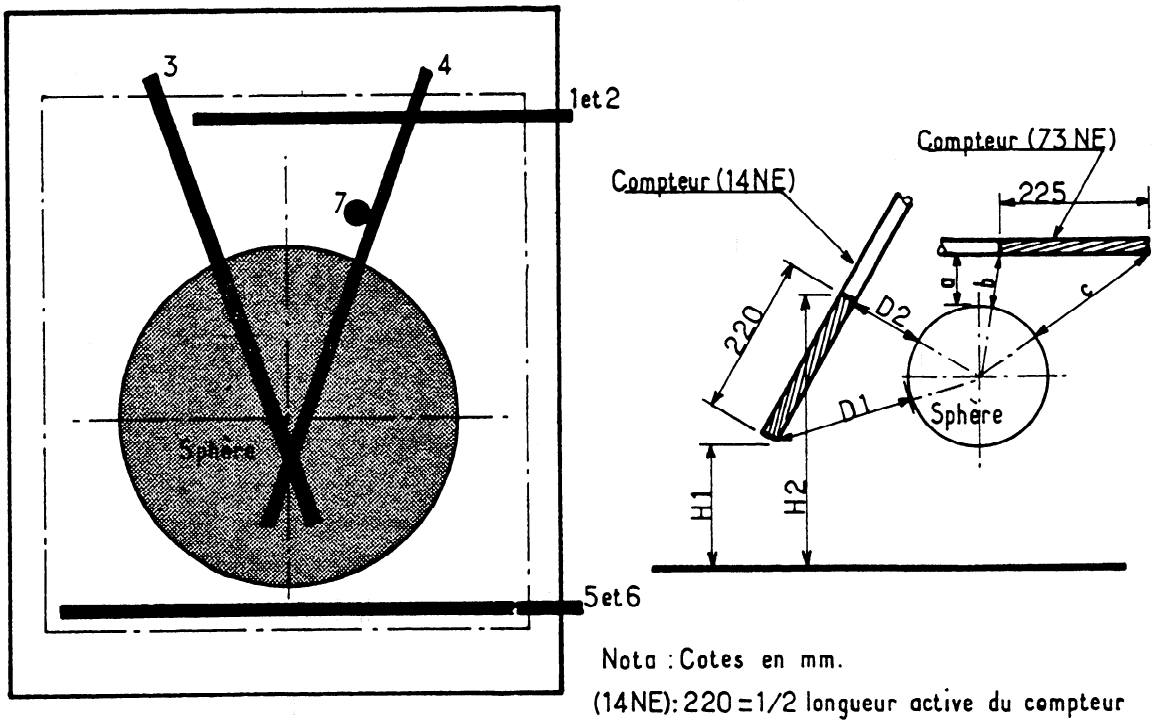

Nota : Cotes en mm.
(14NE): 220 = 1/2 longueur active du compteur
(73NE): 225 = 1/2 longueur active du compteur

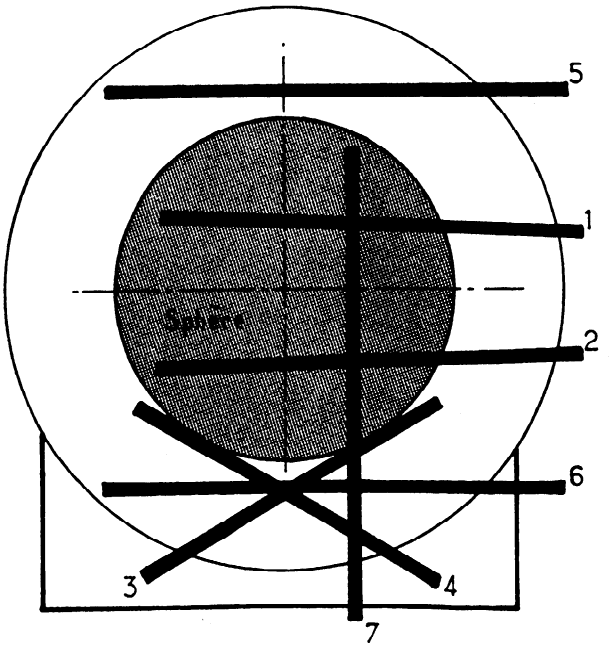

14 NE				
Compteur	H1	H2	D1	D2
C1	900	900	195	155
C2	900	900	195	155
C3	345	530	65	115
C4	430	620	40	100
C5	120	120	170	120
C6	120	120	170	120

73 NE			
Compteur	a	b	c
C7	76	93	685

Fig. 21. Location of the Counters Used with the 510-mm-diam Sphere.

Table 4. Extrapolated Critical Dimensions of Ideal Spheres at the Temperature of the Experiment.

	Nominal Diameter of Spherical Container (mm)									
	540	540	510	510	510	540	510	510	510	540
H:U	5.7	9.9	10.8	11.2	15.2	16.9	21.0	26.0	38	82
T (°C)	89.0	75.0	85.8	75.1	74.8	94.3	74.3	75.0	75.6	75.3
ρ (g/cm^3)	1.92	1.71	1.61	1.63	1.467	1.336	1.321	1.245	1.149	0.973
D_c (mm)	549.5	528	534	521	510.1	537	503	502	502	527
ΔD_c (mm)	0.9	2	2	2	0.5	1	2	2	2	2
V_c (ℓ)	86.9	77	79.8	74.1	69.5	81.0	66.5	66.2	66.2	76.5
ΔV_c (ℓ)	0.4	1	0.7	0.5	0.2	0.4	0.7	0.7	0.8	0.7
$\Delta V_c/V_c$ (%)	0.5	1.3	0.9	0.7	0.3	0.5	1.0	1.0	1.2	0.9

b. a sphere of volume V and hence of diameter $D_1 = \sqrt[3]{\frac{6V}{\pi}}$

c. a sphere having the same surface-to-volume ratio as the truncated sphere of case 1 and hence of diameter

$$D_2 = \frac{6V}{\pi H (2D - H)} .$$

These calculations indicated that the sphere of diameter D_1 is supercritical, the sphere of diameter D_2 is subcritical, and the most probable diameter D_c of a critical sphere lies between D_1 and D_2 according to the relation

$$D_c = D_2 + 0.6(D_1 - D_2)$$

where 0.6 is an empirical quantity derived from DSN calculations.

Following is an example of the transformation of a truncated sphere to an ideal sphere. Starting with the experimental point having an H:U = 9.9 and T = 75°C, the truncated sphere of diameter D = 539.17 mm is critical at a height H = 472.7 mm, corresponding to a volume V = 78.5 ℓ. The diameter D_1 of a sphere of volume V is 531.20 mm; the diameter D_2 of a sphere with the same surface-to-volume ratio as the truncated sphere has a diameter of 523.50 mm. Equation (5) gives D_c = 528.12 mm, which corresponds to a critical volume of 77.13 ℓ.

4.2.3 Critical Dimensions of Ideal Spheres at the Temperature of the Experiment. The critical dimensions listed in Table 4 were obtained from the experimental dimensions by the extrapolation methods thus described. The critical diameter D_c and volume V_c correspond to the temperature T of the experiment.

It was assumed that the absolute error in the critical volume is

$$\Delta V_c = \Delta_1 + \Delta_2$$

where Δ_1 represents the error in the measurement of the volume of the fissile material contained in the sphere. In the case of a full, subcritical sphere, the error Δ_2 in the critical volume due to the extrapolation was estimated from the uncertainty in k_{eff} itself, being due to the uncertainty in the graphic determination of the slope $s\alpha'$. In the case of a truncated critical sphere, it was determined from the

statistical errors in the Monte Carlo calculation that the absolute error Δ_2 in the critical volume V_c due to the extrapolation was less than 2/3 $(V_1 - V_c)$ where V_1 is the volume of a sphere, of diameter D_1, having a volume equal to that of the critical truncated sphere. The value of ΔV_c obtained in this manner seems to be an upper limit. In every case the error $\Delta V_c/V_c$ is less than 1.3%.

From the error ΔV_c, the error in the critical diameter ΔD_c is obtained from

$$\Delta D_c \simeq 2 \frac{\Delta V_c}{\pi D_c^2} .$$

4.2.4 Correlation Between Calculations and Experiments.

4.2.4.1 Computer Programs. The computer programs utilized in these correlations included: (1) the DSN code in the S_4 approximation, based on transport theory, written for an IBM 7094 and using the Hansen-Roach 16-energy-group cross sections;[25] (2) the SECI 01 Monte Carlo code,[26] written for an IBM 7094 and using British cross sections;[27] and (3) the SECI 11 Monte Carlo code[28] written for the IBM 360 and also using the Hansen-Roach 16-energy-group cross sections.

4.2.4.2 Results of Calculations. The values of k_{eff} for ideal critical spheres having dimensions given in Table 4 were calculated by these three programs.

In the materials of these experiments, in which the H:U ratios were relatively low, there is a predominance of epithermal neutrons; thus the 16-group Hansen-Roach cross sections are well suited and no corrections were made in the thermal energy groups.

The Monte Carlo calculations were carried out with 10^4 neutrons (100 neutrons in each of 100 batches); the statistical errors assigned to k_{eff} correspond to a 95% confidence level.

It was necessary to substitute iron for copper in the SECI 01 Monte Carlo calculations because the British cross-section set does not include those of copper. As a consequence these results were systematically too high because of the (n, 2n) reactions in iron; these reactions were eliminated and k_{eff} was recalculated

according to the relation

$$k_{eff} = \frac{\text{total number of fission neutrons}}{\text{total number of initial neutrons}} .$$

The results of these calculations are given in Table 5 and Fig. 22. Table 5 also contains values for a sphere of pure uranium hexafluoride (H:U = 0) for which no experiments were done.

The effect of errors in the experimental data, such as in H:U, density, critical diameter, on the value of k_{eff} may be calculated by the DSN code thus determining the upper limit of the uncertainty in Δk_{eff} given in Table 6. The shaded regions on Fig. 22 indicate the uncertainty in the value of k_{eff} due to experimental errors.

Table 5. Results of Calculations.

H:U	T	ρ (g/cm^3)	D_c (mm)	k_{eff} DSN	k_{eff} SECI 01	k_{eff} SECI 11
5.7	89.0	1.92	549.5	0.993	0.987 ± 0.028	0.965 ± 0.020
9.9	75.0	1.71	528	1.007	1.011 ± 0.026	1.015 ± 0.023
10.8	85.8	1.61	534	1.002	0.992 ± 0.026	0.971 ± 0.024
11.2	85.1	1.63	521	1.006	1.034 ± 0.026	0.982 ± 0.025
15.2	74.8	1.467	510.1	0.996	1.013 ± 0.029	0.981 ± 0.023
16.9	94.3	1.336	537	0.995	1.007 ± 0.023	0.963 ± 0.022
21.0	74.3	1.321	503	0.989	1.007 ± 0.026	0.965 ± 0.023
26.0	75.0	1.245	502	0.975	0.986 ± 0.026	0.968 ± 0.024
38	75.0	1.149	502	0.990	0.995 ± 0.022	0.967 ± 0.022
82	75.3	0.973	527	0.982	0.967 ± 0.027	0.982 ± 0.022
0	75.0	3.63	552.1	1.000	0.998 ± 0.027	1.006 ± 0.020

Table 6. Calculated Errors in k_{eff} Due to Experimental Uncertainties.

H:U	$\Delta k_{eff} \times 10^{-5}$
5.7	~2000
9.9	~1900
10.8	~1100
11.2	~1000
15.2	~ 950
16.9	~1000
21.0	~1100
26.0	~1200
38	~ 600
82	~ 600

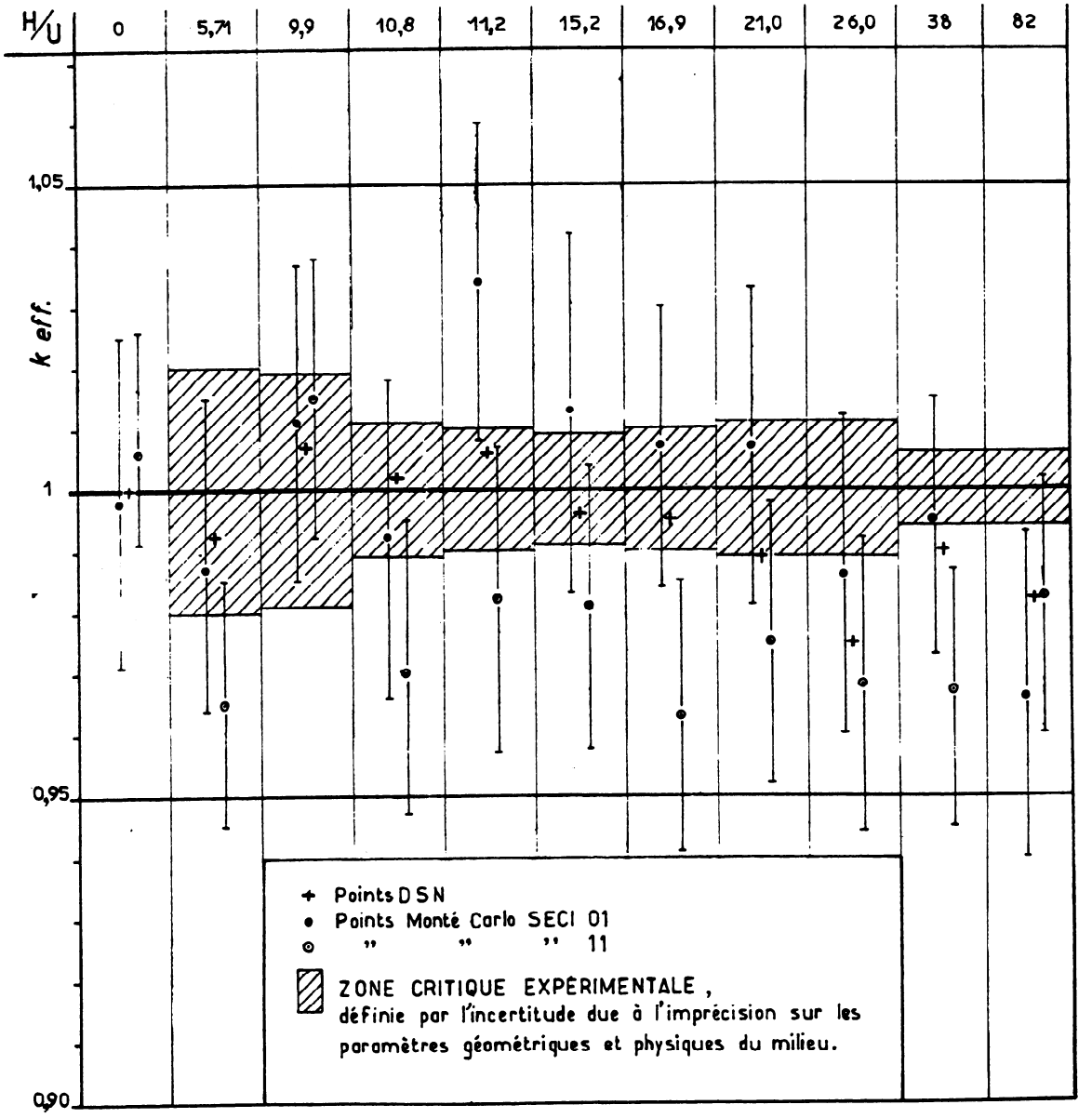

Fig. 22. Comparison of Experimental and Calculational Results.

5. EXTENSION OF THE RESULTS

5.1 Effect of the Container Wall on the Reactivity

The points defining the straight lines in Fig. 23, indicating the variation of k_{eff} as a function of the thickness, e, of the container wall, were calculated by the DSN code. The curves may be summarized as follows:

Material	H:U	$\frac{\Delta k_{eff}}{\Delta e}$ (mm^{-1})
Monel (67% Ni, 3% Fe, 30% Cu; density = 8.80 g/cm^3)	0	-1190×10^{-5}
	20	-1190×10^{-5}
Stainless Steel (72% Fe, 18% Cr, 10% Ni; density = 7.84 g/cm^3)	0	-800×10^{-5}
Pure Aluminum (density = 2.7 g/cm^3)	0	$+146 \times 10^{-5}$

A Monel or a stainless steel wall introduces significant negative reactivity as a result of the relatively large macroscopic absorption cross sections of the alloying components for reflected thermal neutrons. On the other hand, an aluminum wall contributes positive reactivity with respect to a water-reflected sphere without an intervening wall since aluminum is less absorbent than water.

5.2 Effect of the Temperature on the Reactivity

For constant H:U ratio, the density changes in the mixture as a function of temperature may be determined from the family of curves in Fig. 15. The effect of the temperature on the reactivity for two H:U ratios was calculated by the DSN code. For the temperature range examined, 70 to 110°C, these relations are linear as shown in Fig. 24. When

$$H:U = 0, \quad \Delta k_{eff} \simeq -108 \times 10^{-5} \, \Delta T$$

and when

$$H:U = 16, \quad \Delta k_{eff} \simeq -186 \times 10^{-5} \, \Delta T \, .$$

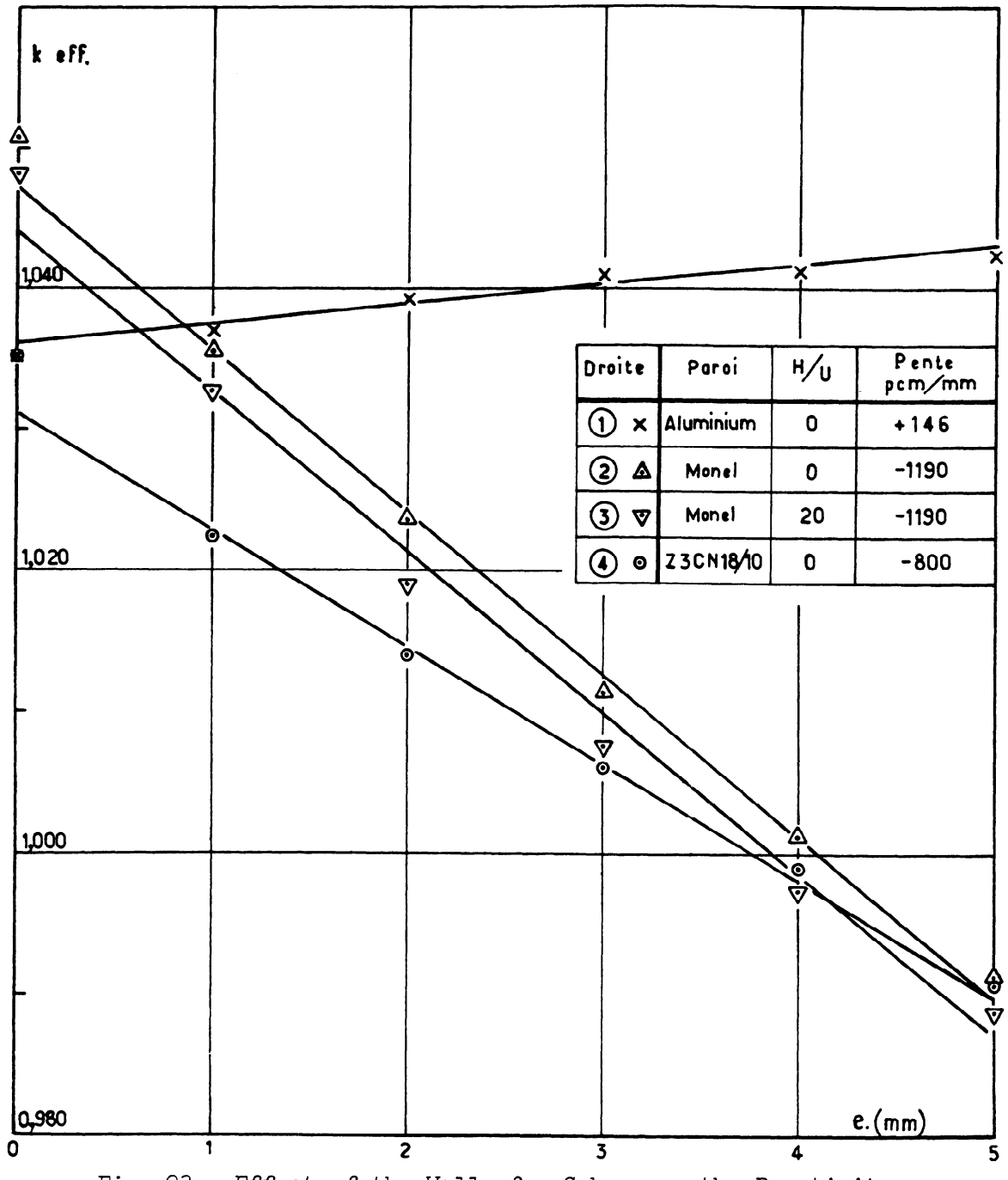

Fig. 23. Effect of the Wall of a Sphere on the Reactivity.

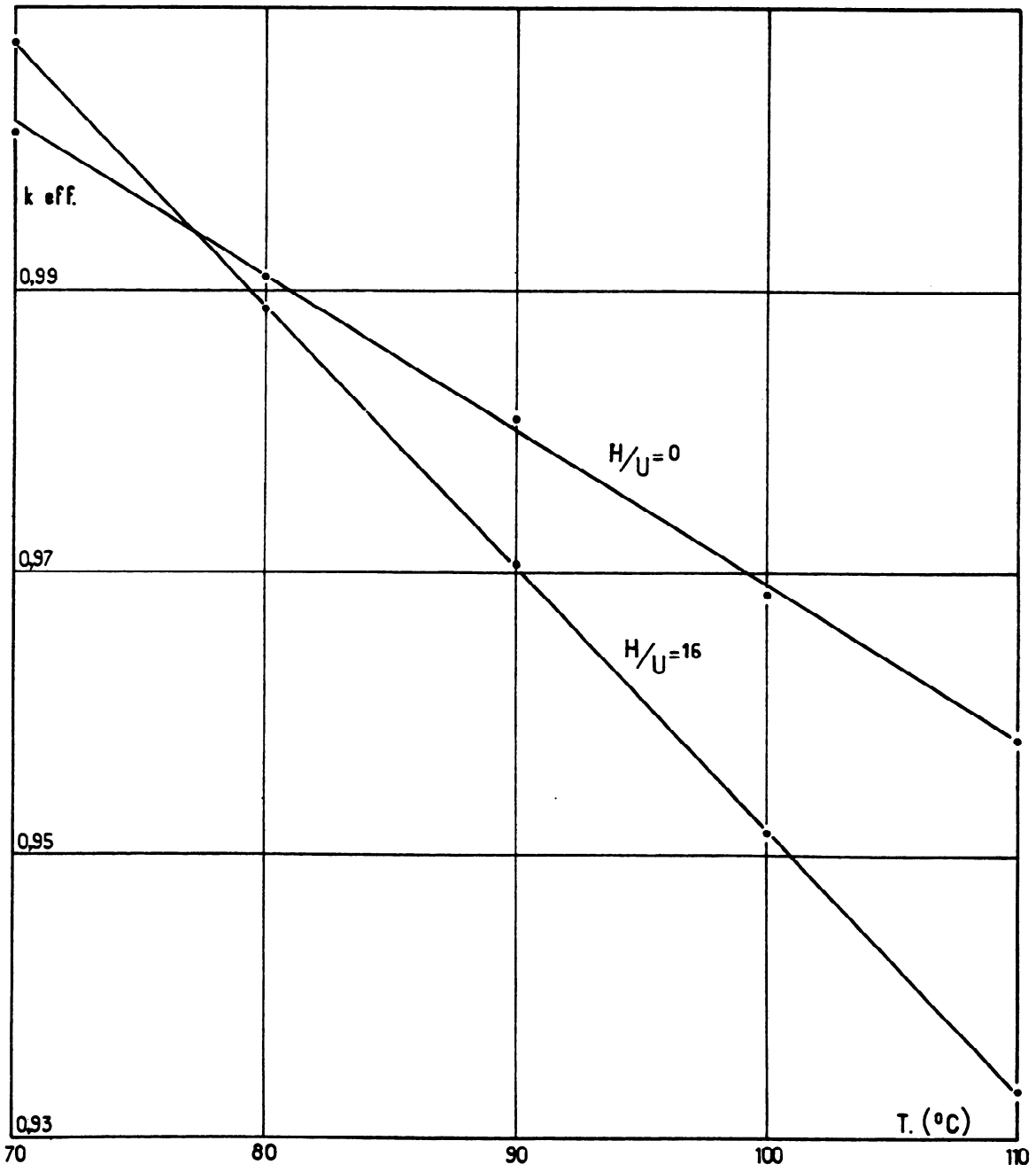

Fig. 24. Effect of the Temperature on the Reactivity at a Constant H:U.

5.3. Critical Spherical Diameters, Volumes, and Masses in a 4-mm-thick Monel Container at 75°C

Since the diameters and volumes of critical spheres given in Table 4 are those established for the varying experimental temperatures, these dimensions were transformed to those appropriate to a temperature of 75°C, which was that most frequent in the experiments.

Knowledge of the effect of a variation in the diameter (Section 4.2.2.1.3) and of the temperature (Section 5.2) on the reactivity permits an adjustment, ΔD, of the critical diameter D_c for the effect of the temperature by

$$\Delta D = \frac{\Delta D}{\Delta k_{eff}} \left(\frac{\Delta k_{eff}}{\Delta T} \right)_{H:U} \Delta T \ .$$

The values for D_c thus obtained and the corresponding critical volumes V_c are given in Table 7 and Fig. 25. The critical volume exhibits a minimum at an H:U ratio near 30.

The density ρ and the H:U ratio of a mixture are experimentally measured quantities. From these values $C_{(U)}$, the uranium concentration may be obtained from the equation

$$C_{(U)} = \frac{(235/349)\ \rho}{(20/349)(H:U) + 1}$$

and the critical mass of the uranium is

$$M_c = C_{(U)}\ V_c \ .$$

The critical mass as a function of uranium concentration is shown in Fig. 26.

The relative uncertainty in the critical mass in terms of the uncertainties in the concentration and the volume was assumed to be

$$\frac{\Delta M_c}{M_c} = \frac{\Delta C_{(U)}}{C_{(U)}} + \frac{\Delta V_c}{V_c} \ .$$

Table 7. Critical Dimensions of UF_6-HF Mixtures as a Function of the H:U Ratio at a Temperature of 75°C. (Uncorrected for 4-mm-thick wall of the Monel container)

H:U	0	5.7	9.9	10.8	11.2	15.2	16.9	21.0	26.0	38	82
ΔH:U		0.1	0.2	0.2	0.2	0.3	0.3	0.4	0.7	2	3
ρ (g/cm^3)	3.63	1.99	1.71	1.65	1.63	1.465	1.413	1.317	1.245	1.140	0.973
$\Delta\rho$ (g/cm^3)		0.015	0.01	0.01	0.01	0.009	0.008	0.008	0.007	0.007	0.006
C (g of U/cm^3)	2.444	1.010	0.74	0.687	0.669	0.527	0.509	0.402	0.337	0.242	0.115
ΔC (g of U/cm^3)		0.015	0.01	0.009	0.009	0.008	0.008	0.0065	0.007	0.010	0.004
D_c (mm)	552.1[a]	537.4	528	523	521	510.4	508	504	502	502	527
ΔD_c (mm)		0.9	2	2	2	0.5	1	2	2	2	2
V_c (liters)	88.1[a]	81.3	77	75.1	74.1	69.6	68.6	67.0	66.2	66.2	76.5
ΔV_c (liters)		0.4	1	0.7	0.5	0.3	0.4	0.7	0.7	0.7	0.7
M_c (kg of U)	215	82	57.0	52	50	36.7	34.9	26.9	22.3	16.0	8.8
$\Delta M_c/M_c$ (%)[b]		2	0.9	1	1	0.7	0.7	0.7	0.7	0.9	0.4
ΔM_c (kg of U)		1.9	1.6	2.1	2.0	1.8	2.1	2.6	3.0	5.4	4.5

a. Calculated by the DSN code.
b. Calculated from the equation of Section 5.3.

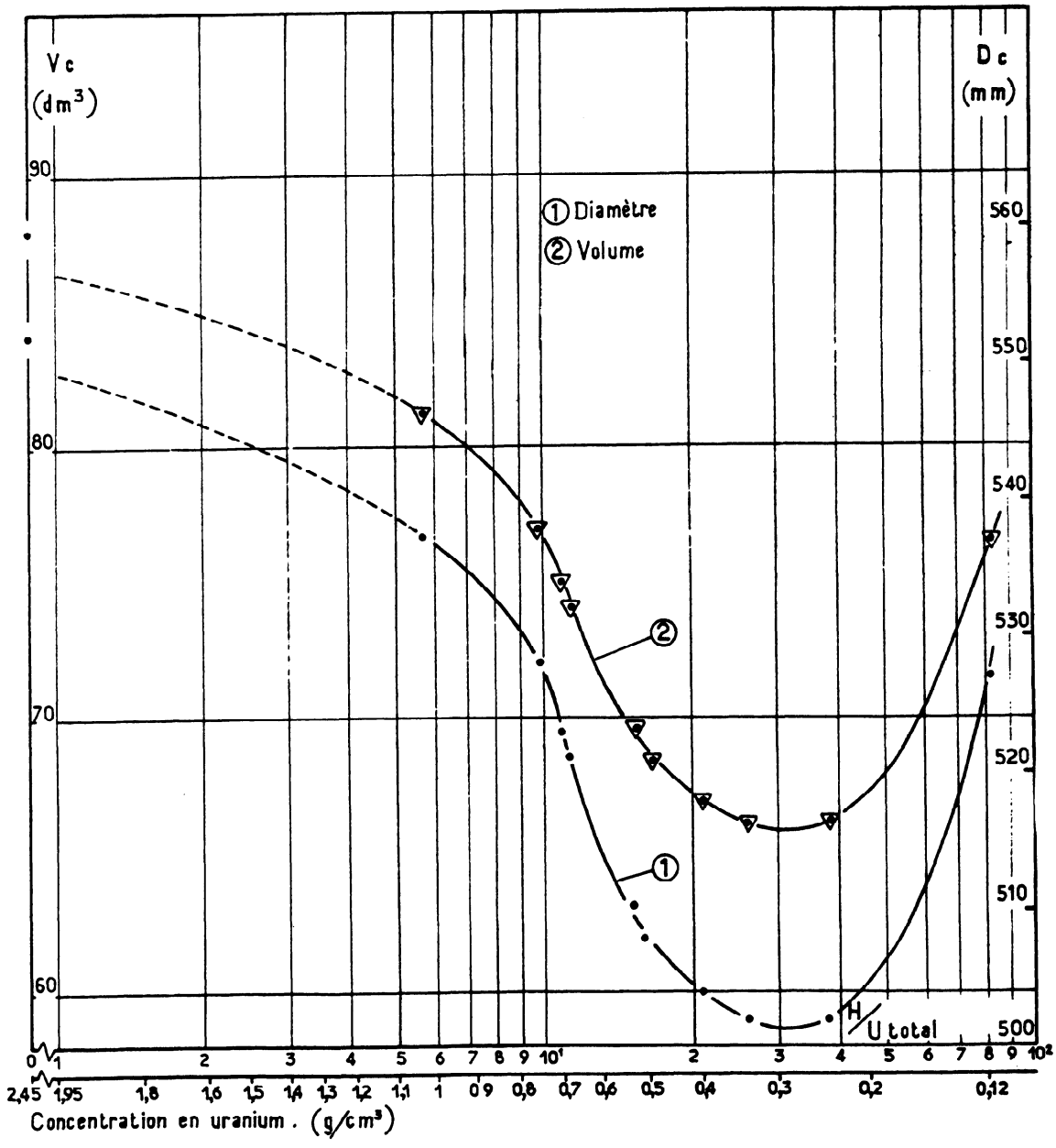

Fig. 25. Critical Diameter and Volume of Liquid UF_6-HF at 75°C as a Function of H:U. The sphere wall was 4-mm-thick Monel.

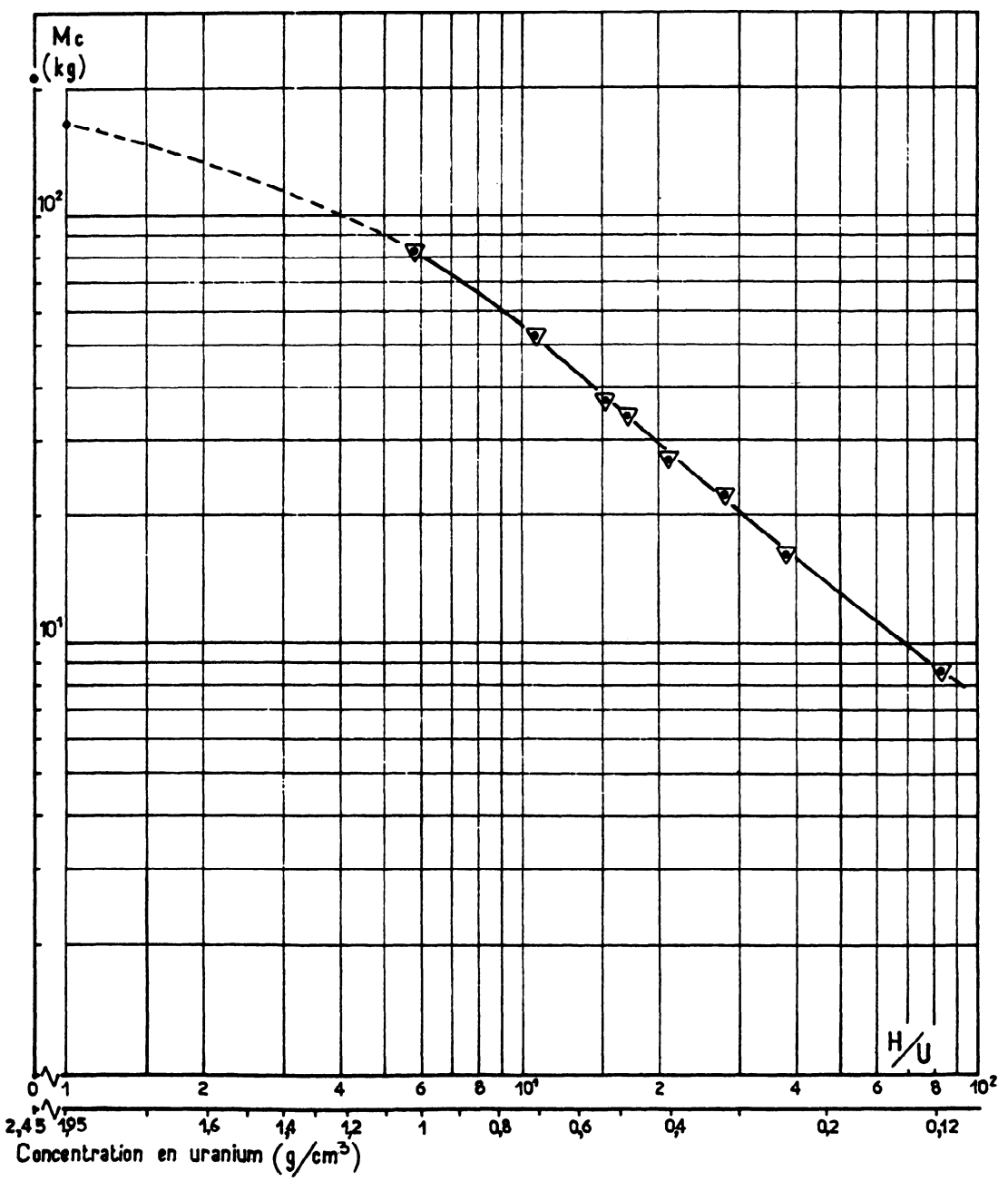

Fig. 26. Critical Mass of Uranium Enriched to 93% in ^{235}U, as Liquid UF_6-HF at 75°C in 4-mm-thick Monel, as a Function of H:U.

The relative error in the volume, $\frac{\Delta V_c}{V_c}$, was taken from Table 4. $\frac{\Delta C_{(U)}}{C_{(U)}}$ was determined from the logarithmic derivative of the expression giving $C_{(U)}$ as a function of density and of H:U as

$$\frac{\Delta C_{(U)}}{C_{(U)}} \leq \frac{\Delta \rho}{\rho} + \frac{(20/349)\,\Delta\,(H:U)}{(20/349)\,(H:U) + 1} \quad .$$

The mean relative error in the critical mass determined in this manner is 2% and it never exceeds 6%.

5.4. Spherical Critical Masses of UF_6-HF in Containers with Infinitely Thin Walls.

The effect of a Monel wall on reactivity was found in Section 5.1 to be -1190×10^{-5} mm^{-1}, independent of the H:U ratio in the range of 0 to 20. The effect of the diameter on the reactivity of a sphere of UF_6-HF was found in Section 4.2.2.1.3 to be 125×10^{-5} mm^{-1}, also independent of the H:U ratio; further, it was assumed that this effect is independent of the wall thickness.

These two effects in combination allow the direct transformation of the critical diameters of ideal spheres with 4-mm-thick Monel walls to the critical diameters of spheres with infinitely thin walls. The curve of critical mass as a function of the H:U ratio, obtained for such spheres, is shown in Fig. 27 for H:U ranges from 0 to 20.

5.5. Spherical Critical Masses of Solutions of UO_2F_2-H_2O

Since Section 4.2.4 indicates that, for H:U ratios up to 20, there is good agreement between the results of the DSN calculations and the experimental data for U-F-H mixtures reflected by water, the DSN code was used to calculate the critical masses of spheres containing UO_2F_2-H_2O (with 93% enriched uranium), at a temperature of 20°C following the standard dilution law,[b] for H:U ratios between 0 and 20. This curve was also plotted on Fig. 27.

---

[b] See, for example, Ref. 23, pp. 954-955.

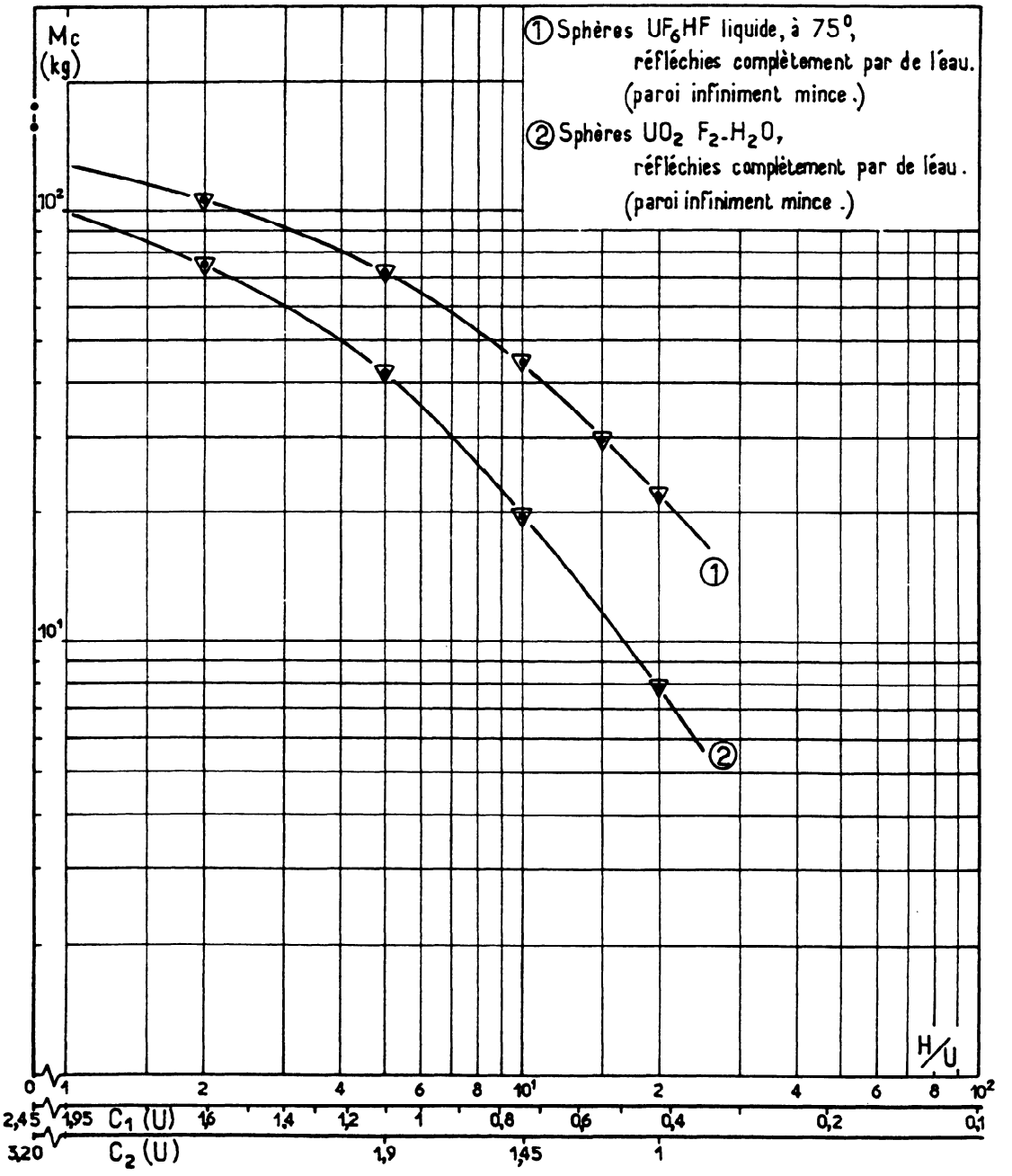

Fig. 27. Critical Mass of Uranium Enriched to 93% in ^{235}U as a Function of H:U.

6. SUMMARY

The engineering and chemical problems posed by the construction and the installation of the experimental equipment have been solved; the operational hazards and the difficulties have been overcome; the experiment yielded relatively good approaches to criticality in a geometry close to that of a true sphere.

The liquid UF_6-HF investigated in these experiments is characterized by its homogeneity, especially at low H:U ratios. For a given H:U ratio, the uranium concentration of this medium is, as far as we know, the lowest one ever studied.

Experimental data obtained for H:U ratios between 0 and 80 allowed the determination, with satisfactory precision, of the critical conditions for liquid UF_6-HF spheres, reflected by 30 cm of water and at a temperature of 75°C. The error in the critical volume is less than 1.3% and the mean error in the critical mass is 2%.

Two sets of conditions whereby UF_6-HF mixtures are subcritical may be deduced from these experiments:

a. A water-reflected, 540-mm-diam sphere of UF_6-HF mixtures of H:U ratio no greater than 5.7 and ^{235}U:U ratio no greater than 0.93 will not be critical provided the temperature of the mixture is 89°C or greater;

b. Water-reflected spheres 450 mm in diameter and smaller containing UF_6-HF mixtures at temperatures of 75°C and over will be subcritical.

Comparison of experimental and theoretical data, obtained by various methods, permits the following conclusions:

a. The DSN transport code yields data that agree well with the experimental results for H:U ratios up to 20; for greater H:U ratios it seems to underestimate k_{eff} by about 1200×10^{-5}.

b. The SECI 11 Monte Carlo code underestimates k_{eff} on the average by 1600×10^{-5}.

c. The SECI 01 Monte Carlo code, after correction for the $(n,2n)$ reactions in iron, yields results that agree well with the experimental data.

Critical masses of uranium, enriched to 93% in ^{235}U, as UO_2F_2-H_2O, were determined by DSN calculations as a function of the H:U ratio between 0 and 20.

REFERENCES

1. Subcommittee 8 of the American Standards Association Sectional Committee N6 and Project 8 of the American Nuclear Society Standards Committee, Nuclear Safety Guide, USAEC Report TID-7016, Rev. 1 (1961).

2. Guide de Criticité, CEA-R3114, Centre d'Études Nucléaires de Saclay (1967).

3. J. H. Chalmers, Handbook of Criticality Data for Plant Designers and Operators, AHSB(S), Handbook 1, United Kingdom Atomic Energy Authority, Risley (1960).

4. C. K. Beck et al., Critical Mass Studies, Part III, K-343, Oak Ridge Gaseous Diffusion Plant (1949).

5. A. D. Callihan et al., Critical Mass Studies, Part IV, K-456, Oak Ridge Gaseous Diffusion Plant (1949).

6. D. Callihan et al., Critical Mass Studies, Part V, K-643, Oak Ridge Gaseous Diffusion Plant (1950).

7. A. H. Snell and J. H. Rush, The Multiplication Factor for Product Drums Containing Uranium Hexafluoride, MonP-47, Monsanto Clinton Laboratories (1945).

8. A. D. Callihan et al., A Test of Neutron Multiplication by Slightly Enriched Uranium, K-740, Oak Ridge Gaseous Diffusion Plant (1949).

9. C. K. Beck, D. Callihan, and R. L. Murray, Critical Mass Studies, Part I, A-4716, Oak Ridge Gaseous Diffusion Plant (1947).

10. C. K. Beck, D. Callihan, and R. L. Murray, Critical Mass Studies, Part II, K-126, Oak Ridge Gaseous Diffusion Plant (1948).

11. S. J. Raffety and J. T. Mihalczo, Homogeneous Critical Assemblies of 2 and 3% Enriched Uranium in Paraffin, Y-DR-14, Union Carbide Corporation, Oak Ridge Y-12 Plant (1969).

12. G. D. Oliver, H. T. Milton, and J. W. Grisard, J. Am. Chem. Soc. 75, 2827 (1953).

13. Ferdinand G. Brickwedde, Harold J. Hoge, and Russell B. Scott, J. Chem. Phys. 16, 429 (1948).

14. Bernard Weinstock and John G. Malm, Some Recent Studies with Hexafluorides, Proc. of the Second United Nations International Conference on the Peaceful Uses of Atomic Energy, Conference de GENEVE 1958 28, 125 (1959).

15. D. R. Llewellyn, J. Chem. Soc. of London, Pt. 1, 28 (1953).

16. J. H. Awbery, The Vapor Pressure of Solid UF_6, BR-302, Imperial Chemical Industries, Ltd. (1943).

17. R. Dewitt, Uranium Hexafluoride: A Survey of the Physico-Chemical Properties, GAT-280, Goodyear Atomic Corporation (1960).

18. J. Vicard, Monographie sur UF_6, Laboratorie de Recherches de Lyon, Société UGINE-PIERRE BENITE (Rhône) (1956).

19. P. Pascal, Nouveau Traité de Chimie Minérale, Tome XVI, Fluor, Chlore, Brome, Iode, Astate ..., Masson et Cie, Paris (1960).

20. I. E. Ryss, The Chemistry of Fluorine and Its Inorganic Compounds, Parts 1 and 2, AEC-tr-3927 (1960). Original published by State Publishing House for Scientific, Technical, and Chemical Literature, Moscow (1956).

21. G. P. Rutlege, R. L. Jarry, and W. Davis, Jr., J. Phys. Chem. 57, 541 (1953).

22. R. L. Jarry, F. D. Rosen, C. F. Hale, and Wallace Davis, Jr., J. Phys. Chem. 57, 905 (1953).

23. Samuel Glasstone, Textbook of Physical Chemistry, Second Edition, p. 753, D. Van Nostrand Company, Inc. (1946).

24. C. Clouet D'Orval, E. Deilgat, M. Houelle, and P. Lecorche, La Recherche Experimentale Francaise en Matiere de Criticite, Criticality Control of Fissile Materials, p. 193, Proc. of a Symposium, Stockholm, 1-5 Nov. 1965, International Atomic Energy Agency, Vienna (1966).

25. Gordon E. Hansen and William H. Roach, Six and Sixteen Group Cross Sections for Fast and Intermediate Critical Assemblies, LAMS-2543, Los Alamos Scientific Laboratory (1961).

26. J. Moreau, H. Rabot, and Cl. Robin, Méthode de Monte-Carlo: Codes pour l'Etude des Problemes de Criticité (IBM 7094), CEA-R-2872, Centre d'Etudes Nucléaires de Saclay (1965).

27. K. Parker, The Aldermaston Nuclear Data Library as of May 1963, AWRE Report Nr 0-70/63, United Kingdom Atomic Energy Authority (1963).

28. J. Moreau and R. Pouches, personal communication (1968).